Journal of Quantitative Spectroscopy & Radiative Transfer 229 (2019) 145–156

Contents lists available at ScienceDirect

Journal of Quantitative Spectroscopy & Radiative Transfer

journal homepage: www.elsevier.com/locate/jqsrt

Observation and interpretation of the $5p^5 4f^3 5d$ core-excited configuration in triply ionized neodymium Nd^{3+} (Nd IV)

Kamel Arab[a], Djamel Deghiche[a], Ali Meftah[a,b], Jean-François Wyart[b,c], Wan-Ü Lydia Tchang-Brillet[b,*], Norbert Champion[b], Christophe Blaess[b], Omar Lamrous[a]

[a] Laboratoire de Physique et Chimie Quantique, Université Mouloud Mammeri, BP 17 RP, Tizi-Ouzou 15000, Algérie
[b] LERMA, Observatoire de Paris-Meudon, PSL Research University, CNRS UMR8112, Sorbonne Université, Meudon F-92195, France
[c] Laboratoire Aimé Cotton, CNRS UMR9188, Univ Paris-Sud, ENS Cachan, Univ Paris-Saclay, bâtiment 505, Orsay CEDEX 91405, France

ARTICLE INFO

Article history:
Received 22 October 2018
Revised 6 February 2019
Accepted 26 February 2019
Available online 7 March 2019

Keywords:
Atomic spectra
Transitions
Energy levels
Lanthanide ions

ABSTRACT

Ultraviolet laboratory observation of the emission spectrum of the triply ionized neodymium Nd IV excited in a vacuum spark source was extended to shorter wavelength region down to 350 Å. The present analysis, based on the identification of 313 spectral lines, led to the determination of 125 previously unknown energy levels, all but two belonging to the core-excited configuration $5p^5 4f^3 5d$ in the Nd^{3+} ion. Theoretical calculations of even parity configurations were performed by using the parametric Slater-Racah method including configuration interactions. Energy parameter values were fitted by least-squares with a root-mean-square (rms) deviation of 184 cm^{-1} for an average energy $E_{av}(5p^5 4f^3 5d) = 221\,076\ cm^{-1}$. In this work, we quantitatively confirm the effect of reduction of the $5p^6 4f^3$ - $5p^6 4f^2 5d$ transition probabilities by the configuration interaction between $5p^6 4f^2 5d$ and core-excited $5p^5 4f^3 5d$ configurations, which is similar to the one observed in Nd V for the $5p^6 4f^2$ - $5p^6 4f5d$ transitions.

1. Introduction

Structures and spectroscopic properties of lanthanide ions are of interest in many aspects relevant for laboratory and astrophysical plasmas. The earliest compilation of their energy levels was published by Martin *et al* in 1978 [1]. More recent bibliography on their spectroscopic data can be found in the database maintained by NIST [2]. One may recall that the lanthanides are incorporated into crystals, fibers or glass ceramics as trivalent ions for various applications involving their optical properties (See for example ref [3]). In astrophysics singly and doubly charged ions of lanthanides have been detected in Hubble Space Telescope observations of the atmospheres of chemically peculiar stars (See for example ref [4]). More recently, detection of neutron star mergers by simultaneous emission of gravitational waves and electromagnetic emission, with the predictions on formation of heavy elements in the ejected matter, strengthens the interest for radiative properties of ions up to triply charged [5].

Among all the lanthanides, neodymium has always attracted special attention, if only for the well known laser line at 1064 nm emitted by Nd^{3+} ions embedded in crystals. About a decade ago, analyses of the free ion Nd^{3+}(Nd IV) was carried out based on high-resolution emission spectra of vacuum spark sources [6,7].

The ground-state configuration of the Nd^{3+}ion (Nd IV) is built on three valence electrons $4f^3$. The spectrum belongs to the lanthanum (La I) isoelectronic sequence. In an earlier work [7], a number of 1426 identified lines in the wavelength range of 1160 - 2800 Å led to the complete determination of all 41 levels of $5p^6 4f^3$ and 191 levels of the lowest excited configurations $5p^6 4f^2 5d$, $4f^2 6s$ and $4f^2 6p$. The same set of spectrograms also contained emission lines from the Nd^{4+} ion (Nd V). The subsequent analysis of the Nd V spectrum [8] reported the complete determination of the ground-state configuration $5p^6 4f^2$ (except for $^1S_0$), and the lowest excited configurations $5p^6 4f5d$, 4f6s and 4f6p, altogether with the identification of 250 spectral lines in the range of (700–2240 Å).

In the parametric calculations performed for interpretation of the Nd IV [7] and Nd V [8] spectra, configuration interactions with core-excited configurations, respectively $5p^5 4f^3 5d$ in Nd IV and $5p^5 4f^2 5d$ in Nd V, were taken into account and showed to have influence on the intensities of observed 4f - 5d resonance transitions by reducing them. However, the corresponding interaction parameters could only be fixed to appropriate estimated values in the least-squares fits of energy levels in both ions, in absence of any experimental levels of these higher configurations. Later on, based on the same set of existing experimental level energies [7], transition probabilities for allowed and forbidden lines in Nd IV

* Corresponding author.
E-mail address: lydia.tchang-brillet@obspm.fr (W.Ü.L. Tchang-Brillet).

https://doi.org/10.1016/j.jqsrt.2019.02.031
0022-4073/

were investigated by Enzoga Yoca and Quinet [9], who performed similar parametric calculations with a larger basis of configurations and including explicitly more configuration interactions. Comparing their gA values of electric dipole lines with the values from the previous work [7], the authors estimated a good agreement of within %25. They also mentioned the influence of core-excited configurations leading to a reduction of transition probabilities of resonance lines by a factor of about 2. This was consistent with the fact that lifetimes derived from both parametric calculations [7,9] for some $5p^64f^25d$ levels were about two times longer compared to those calculated by Dzuba et al. [10] without taking into account core-excited configurations (Cf Table 4 [9]). Such effect on the 4f - 5d resonance line intensities was furthermore studied in the case of Tm IV [11] where the $5p^54f^{11}$ and $5p^54f^{12}5d$ configurations were introduced into their respective parities in the parametric calculations. However, again, no available experimental energy levels of the Tm^{3+} ion could be used to fit the corresponding configuration interaction parameters.

The first laboratory observation of core-excited configurations was reported by Reader and Wyart [12] for Ce^{3+} (Ce IV). In the parametric interpretation, 68 and 21 experimentally determined levels belonging respectively to the $5p^54f5d$ and $5p^54f6s$ configurations were introduced. The authors established that the interaction of these configurations with the $5p^6nd$ series resulted in a large fine structure splitting of the 6d ^{2}D term. They also pointed out a reduction of transition probabilities of the 4f - 5d resonance lines by a factor of nearly 2 because of interaction between $5p^65d$ and $5p^54f5d$. Recently, by extending the experimental observation of ionized neodymium to shorter wavelengths down to 370 Å, the core-excited configuration $5p^54f^25d$ in the Nd^{4+} ion (Nd V) was observed and interpreted [13]. Consequently the effect of reduction of transition probabilities of the $5p^64f^2$ - $5p^64f5d$ transition array by the $5p^64f5d$ - $5p^54f^25d$ configuration interaction was made clear and quantitative in Nd V [13].

The main objective of the present work was to study similar effects in triply ionized neodymium Nd^{3+} (Nd IV), by extending the previous analysis [6,7] to the short wavelength range of 400–600 Å, aiming to determine energy levels of the core-excited $5p^54f^35d$ configuration by their transitions to the $5p^64f^3$ ground-state configuration and to quantitatively confirm the strong reduction of the $5p^64f^3$ - $5p^64f^25d$ transition probabilities by the $5p^64f^25d$ - $5p^54f^35d$ configuration interaction. Fig. 1 displays a diagram of transitions between configurations of Nd IV that were involved in the present work. Note that mixing may occur between the two overlapping core-excited configurations $5p^54f^35d$ and $5p^54f^36s$.

2. Experiment and line list

The spectrograms used in previous publications on neodymium ion spectra [6–8,13] contain emission lines from Nd^{3+} and Nd^{4+} at the same time. They are therefore used again in the present work. Experimental details can be found in previous publications [6–8,13]. Here we only recall the main features. At the early stage of the work, we had at our disposal two sets of recordings using two sliding spark sources: one in the wavelength range of 390–2700 Å from the National Bureau of Standards (NBS) with photographic plates (PP) (10.7m normal incidence spectrograph with 1200 lines mm^{-1} concave grating, plate factor 0.78 Å mm^{-1} in the first order); the second in the range of 700–1000 Å from the 10.7 m vacuum ultraviolet normal incidence spectrograph of the Meudon Observatory (3600 lines mm^{-1} holographic concave grating, plate factor of 0.26 Å mm^{-1}), either on photographic plates or on phosphor storage image plates (IP). The latter (Fuji BAS-TR 2040) were digitized by a specific scanner FUJI9000 at a sample step of 10 microns and had a linear response over five orders of magnitude in intensity measurements. As for the photographic spectra, they were digitized by a high-resolution optical scanner iQsmart1 simultaneously with an optical ruler for the correction of a possible non-linearity in displacements, as explained in the recent article on Yb V [14]. In the measurement software, an experimental intensity with arbitrary units could be estimated for each line from the area of a triangle fitting the line profile.

The transition arrays connecting core-excited configurations to the ground-state configurations in Nd V and Nd IV were predicted to occur at wavelengths shorter than 500 Å and 600 Å respectively, overlapping each other. We extended the wavelength measurements on the spectrum from NBS PP down to 393 Å and calibrated it with internal reference lines emitted by low Z impurities like C, N, O ions [15]. However, internal references became scarce for wavelengths shorter than 450 Å. More spectra were thus recorded in Meudon, either with the same sliding spark source as used in [6,7] in the range of 440–650 Å or with a three-electrode triggered spark source for the range of 350–555 Å, with a similar setting as described in the W VIII study [16]. Alternatively to the pure neodymium anode, an anode in a Nd/Fe/B alloy was mounted, producing ionized iron lines, of which the newly compiled Fe V Ritz wavelengths [17] were used for calibration. The uncertainty on measured wavelengths could be estimated to be around ± 0.005 Å for isolated lines. Some blends were unavoidable, given the density of lines reaching 10 lines per Angström.

3. Analysis and determination of energy levels

The present analysis was supported by theoretical calculations applying the Slater-Racah method [18] performed with Cowan's code package (RCN/RCN2/RCG/RCE) [19] in its WINDOWS version [20]. A first *ab initio* step was given by a relativistic Hartree-Fock (HFR) calculation using the RCN code, followed by the calculation of energy parameters P_{HFR}, i.e. electrostatic and spin-orbit radial integrals, including CI integrals, by the RCN2 code. These ab initio values of P_{HFR} were then scaled for obtaining the input data of the diagonalization code RCG. Generally, the initial scaling factor (SF) defined as $SF=P_{fit}/P_{HFR}$ could be estimated from neighboring spectra by regularities. In the present case, the Hamiltonian was diagonalized for the odd parity with the same basis as in the previous work on Nd IV [7]: one core-excited configuration $5p^54f^4$ and five closed 5p sub-shell $5p^64f^3$, $5p^64f^26p$, $5p^64f(5d+6s)^2$. For the even parity, the basis included two closed 5p sub-shell configurations $5p^64f^25d$ and $5p^64f^26s$ and was extended by adjoining one more open shell configuration, $5p^54f^36s$, to $5p^54f^35d$. The initial SF values for most of the parameters were their final values from the previous parametric study [7], fitted against experimentally known level energies. For parameters involving the inner $5p^5$ subshell, results on Ce IV [12] provided improved initial SF values. The ab initio HFR average energies of different configurations E_{av} were corrected by estimates from the experimental spectrum, in particular from the positions of the strongest emission arrays.

The search of energy levels was guided by these preliminary estimations. Then we applied the Ritz combination principle and, at the same time, we ensured the consistency between observed spectral lines intensities and theoretical transition probabilities gA. As soon as some experimental level energies became known, we iteratively ran the RCE code where the radial integrals were considered as adjustable parameters P_{fit} in a least-squares fit minimizing the differences between calculated and experimental energies. The procedure was followed until convergence. The last least-squares fit provided the final parameter values for deriving the level compositions, Landé factors and transition probabilities in the RCG code.

The analysis was helped by using the IDEN code [21,22] which allowed for a great amount of theoretical and experimental data to be visualized simultaneously. On the display screen in IDEN, chains

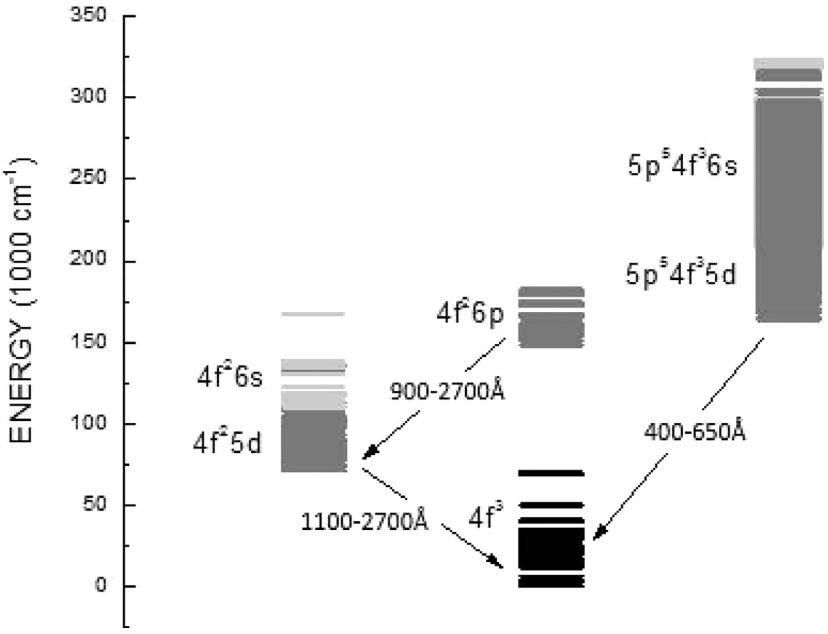

Fig. 1. Transition diagram of Nd^{3+}. The longer wavelength region was investigated previously [7]. The shorter one is studied in the present work.

of transitions involving a common level appeared as more or less well defined alignments.

4. Results and discussion

In the present work, the search of levels of the core-excited $5p^54f^35d$ configuration was based on their transitions to the ground-state configuration $5p^64f^3$. Overall a number of 313 spectral lines between 397 and 635 Å were identified and 125 previously unknown excited energy levels were determined. All but two levels belong to the $5p^54f^35d$ configuration. The remaining two levels have main components belonging to the $5p^54f^36s$ configuration. Due to configuration mixings and intermediate coupling, there are two cases where a $5p^54f^35d$ level has many small components among which the leading term is a $5p^54f^36s$ term. The level compositions are very sensitive to small changes in energy parameters. Therefore only the energy value and the quantum number J characterize an energy level unambiguously.

The final classified lines for $5p^64f^3$-$5p^54f^35d$ (or 6s) transitions of Nd IV are reported in Table 1, together with the gA values and the corresponding cancellation factors (CF) as defined by equation (14.107), p 432 in [19], derived from the parametric calculations (See Table 3). In Table 1, each transition is identified by its lower and upper levels (See Table 2). Since more lines were seen in the NBS spectrum in the overlapping region (448 - 636 Å) of NBS photographic plates and Meudon image plates, the listed lines with their intensities in Table 1 are from IP between 397–448 Å and from PP between 448 - 636 Å.

The classified lines, as outputs of IDEN code, provided the input for the LOPT code [23], which carried out an iterative optimization process of the energy values by minimizing the differences between the observed wave numbers of spectral lines and those calculated by the Ritz principle from the experimental level energies. All the level energies of the ground-state configuration $5p^64f^3$ were fixed to their values found in [7]. In Table 2, we present the optimized values of 125 level energies of the $5p^54f^35d$ (or $5p^54f^36s$) configuration with their uncertainties, their quantum numbers J and the number of transitions to the levels of the opposite parity involved in their determination. The procedure of optimization of level energies in LOPT [23] included implicitly the optimization of Ritz wavelengths. These are compared with measured wavelengths in Table 1, along with their uncertainties as estimated in LOPT.

Two strong transition arrays appeared around 415 and 480 Å for the $5p^64f^3$ - $5p^54f^35d$ transitions. Similar to the Nd V case [13], this structure reflects the structure of the $5p^6\ ^1S$ - $5p^55d\ ^1P$ and $5p^6\ ^1S$ - $5p^55d\ ^3P$ or ^3D transitions in the presence of the three $4f^3$ spectator electrons. The ^1P term lies above the other terms of the $5p^55d$ configuration because of the large value of the Slater exchange integral $G^1(5p, 5d)$ and generates the transition array from the upper part of the $5p^54f^35d$ configuration, which is localized around the shortest wavelength of 415Å. A small amount of mixtures between the levels $^1P_1$ - $^3P_1$ and $^1P_1$ - $^3D_1$ generate transitions from the lower part of $5p^54f^35d$, which are localized around 480 Å. In IDEN, alignments with several (three to six) transitions around 480 Å were observed for energies between 180 000 and 235 000 cm^{-1}, the lower part of the configuration, whereas lines around 415 Å often show alignments with only two strong transitions from the higher part of the configuration.

For the odd-parity configurations including the ground-state configuration $5p^64f^3$, the parametric calculations led to the same final parameter values as in [7]. The corresponding results on level compositions were used for the present calculations of transition probabilities.

For the even parity, the diagonalization of Hamiltonian matrix of the four configurations involved a maximum size of 453x453, corresponding to J = 7/2. Table 3 reports the set of energy parameters from the final iteration of the least-squares fit in the RCE code, including the 125 levels identified in this work and the 121 levels of $5p^64f^25d$ and $5p^64f^26s$ determined previously in [7]. In Table 3, the fitted parameter values, as well as their uncertainties from the fit, are displayed. HFR values of the parameters and the corresponding $SF=P_{fit}/P_{HFR}$ are listed for comparison. For the average energy E_{av} of a configuration, the difference between fitted and HFR values is given in the column SF. A number of 92 parameters was involved, which included Slater parameters R^k for the first-order configuration interactions (CI) and effective parameters for the second order perturbations from far configurations, such as α, β, γ and the "Slater forbidden" parameters $F^1(fd)$, $G^2(fd)$, $G^4(fd)$ for non-equivalent electrons [19].

Table 1
Observed lines identified as the $5p^64f^3$ -$5p^54f^35d$ transitions in Nd IV. Experimental intensities in arbitrary units ; calculated transition probabilities gA, g being the statistical weight of the upper level, with a 10-configuration basis. CF is the cancellation factor defined by equation (14.107), p432 in [19]. λ_{Ritz} is derived from the level energies as $\lambda_{Ritz}(\text{Å}) = (E_{up} - E_{low})^{-1}$; $\delta\lambda_{Ritz}$ is its uncertainty as estimated in LOPT [23]. $\Delta\lambda = \lambda_{exp} - \lambda_{Ritz}$. All energies and wave numbers are in cm^{-1}. The comments after the wavelengths are explained in footnotes at the end of the table. The energy levels are labelled by their first LS component (Cf Table 2 for upper levels and [7] for lower levels).

λ_{exp}(Å)	Int_{exp}	$gA(s^{-1})$	CF	λ_{Ritz}(Å)	$\delta\lambda_{Ritz}$(Å)	$\Delta\lambda$(Å)	Lower level label	E_{low}	Upper level label	E_{up}
397.257	14	1.50E+10	0.34	397.262	0.003	−0.005	p6f3 4G 5.5	22 047.39	p5f3d 4D4Fe 4.5	273 770.7
400.786	7	2.60E+10	0.23	400.776	0.003	0.010	p6f3 4F 4.5	14 994.87	p5f3d 4G4Fc 4.5	264 511.1
401.363	34	3.04E+10	0.09	401.364	0.003	−0.001	p6f3 2K 7.5	22 043.77	p5f3d 2L2Le 7.5	271 194.2
404.099	28	1.75E+11	0.75	404.104	0.002	−0.005	p6f3 2L 7.5	31 036.00	p5f3d 2H2I1$_b$ 6.5	278 497.2
405.377	24	6.99E+10	−0.48	405.371	0.002	0.006	p6f3 2I 6.5	31 582.85	p5f3d 2H2I1$_b$ 5.5	278 270.7
406.563	38	1.58E+11	−0.91	406.557	0.004	0.006	p6f3 2I 6.5	31 582.85	p5f3s 2L4L 7.5	277 550.8
406.960	38	6.88E+10	−0.54	406.951	0.003	0.009	p6f3 2I 6.5	31 582.85	p5f3d 2H2H1 5.5	277 312.8
407.570	25	8.65E+09	−0.11	407.562	0.003	0.007	p6f3 2H2 5.5	16 161.53	p5f3d 2K2Ke 6.5	261 522.8
408.179	34	2.28E+11	−0.45	408.185	0.004	−0.006	p6f3 2L 8.5	32 563.57	p5f3s 2L4L 7.5	277 550.8
408.932	14	2.05E+11	−0.49	408.949	0.002	−0.017	p6f3 2H1 4.5	33 741.15	p5f3d 2H2I1$_b$ 5.5	278 270.7
409.311	19	3.69E+10	−0.45	409.318	0.003	−0.007	p6f3 2H2 5.5	16 161.53	p5f3d 2G4H2 4.5	260 470.3
409.775	26	3.38E+11	−0.82	409.775	0.005	0.001	p6f3 2F2 2.5	39 568.42	p5f3d 2F2D1 1.5	283 605.0
410.022bl	18	2.46E+10	−0.25	410.0188	0.0023	0.003	p6f3 4I 6.5	3907.43	p5f3s 4I4Kb 6.5	247 798.7
410.144bl	39	7.28E+11	−0.75	410.144	0.005	−0.001	p6f3 2G1 4.5	49 172.45	p5f3d 2G2G2 4.5	292 989.0
410.358	35	2.81E+11	−0.70	410.365	0.004	−0.006	p6f3 2H1 4.5	33 741.15	p5f3d 2H2H1 4.5	277 426.8
410.552	25	2.94E+11	0.80	410.557	0.003	−0.005	p6f3 2H1 4.5	33 741.15	p5f3d 2H2H1 5.5	277 312.8
410.589	26	2.55E+10	0.11	410.589	0.004	0.000	p6f3 2D2 1.5	34 275.21	p5f3d 2D2D2 2.5	277 827.9
410.687	34	4.41E+11	−0.67	410.687	0.005	0.000	p6f3 2H1 5.5	35 136.61	p5f3d 2H2G1 4.5	278 631.0
410.791	34	7.76E+10	0.14	410.801	0.004	−0.011	p6f3 4D 2.5	29 190.91	p5f3d 4D4Df 3.5	272 617.7
410.832	25	1.17E+11	0.38	410.832	0.005	0.000	p6f3 2F2 3.5	41 012.70	p5f3d 2F2G1 4.5	284 421.0
410.918	46	8.98E+11	−0.85	410.913	0.002	0.005	p6f3 2H1 5.5	35 136.61	p5f3d 2H2I1$_b$ 6.5	278 497.2
410.990	28	4.56E+11	−0.81	410.990	0.005	0.000	p6f3 2F2 3.5	41 012.70	p5f3d 2F2D1 2.5	284 327.7
411.174	32	4.31E+11	−0.87	411.166	0.004	0.007	p6f3 2K 6.5	20 005.22	p5f3d 2K2If 5.5	263 215.7
411.306bl	40	5.00E+11	−0.85	411.296	0.002	0.011	p6f3 2H1 5.5	35 136.61	p5f3d 2H2I1$_b$ 5.5	278 270.7
411.486	32	3.69E+10	0.20	411.493	0.003	−0.007	p6f3 2G2 4.5	21 493.39	p5f3d 4G4Fc 4.5	264 511.1
411.526	45	2.91E+10	0.24	411.532	0.004	−0.006	p6f3 4G 3.5	19 540.80	p5f3d 4G4Ff 3.5	262 535.2
411.681	62	1.55E+11	0.89	411.683	0.003	−0.002	p6f3 2K 6.5	20 005.22	p5f3d 4G4Ge 5.5	262 910.4
411.828	35	9.51E+10	0.44	411.836	0.003	−0.007	p6f3 2G2 3.5	17 655.11	p5f3d 2G4H2 4.5	260 470.3
411.996	67	7.21E+11	−0.88	411.998	0.004	−0.002	p6f3 2I 5.5	30 179.93	p5f3d 2I2Kd 6.5	272 899.7
412.178	34	3.02E+11	0.71	412.177	0.004	0.000	p6f3 2D2 2.5	35 213.92	p5f3d 2D2D2 2.6	277 827.9
412.266	51	1.99E+11	−0.67	412.260	0.004	0.006	p6f3 4G 4.5	19 969.79	p5f3d 4G4Ff 3.6	262 535.2
412.430	89	5.52E+11	0.86	412.433	0.003	−0.002	p6f3 4G 5.5	22 047.39	p5f3d 4G4Fc 4.5	264 511.1
412.519	53	6.15E+11	0.92	412.515	0.004	0.004	p6f3 4D 3.5	31 355.04	p5f3d 4D4Fe 4.6	273 770.7
412.657blV	60	7.07E+11	−0.86	412.660	0.004	−0.003	p6f3 2I 6.5	31 582.85	p5f3d 2I2Ie 6.5	273 912.9
412.734blV	45	4.77E+10	0.26	412.728	0.004	0.006	p6f3 2H1 5.5	35 136.61	p5f3d 2H2H1 4.5	277 426.8
412.874	65	5.64E+11	−0.81	412.869	0.003	0.005	p6f3 2I 5.5	30 179.93	p5f3d 2I2Hf 4.5	272 387.5
412.919	71	4.28E+11	−0.54	412.923	0.003	−0.004	p6f3 2H1 5.5	35 136.61	p5f3d 2H2H1 5.5	277 312.8
412.967	51	4.81E+11	0.91	412.967	0.005	0.000	p6f3 2D2 1.5	34 275.21	p5f3d 2D2F2 2.5	276 425.4
413.059	63	6.88E+11	−0.87	413.060	0.003	−0.001	p6f3 2I 6.5	31 582.85	p5f3d 2I2Hf 5.5	273 678.6
413.151	84	3.55E+11	−0.71	413.148	0.004	0.003	p6f3 4G 3.5	19 540.80	p5f3d 4G4Ge 3.5	261 585.0
413.264	38	1.44E+10	0.32	413.2662	0.0018	−0.002	p6f3 4I 4.5	0.00	p5f3d 2I4Gb 4.5	241 974.8
413.366	69	2.81E+11	0.78	413.364	0.004	0.002	p6f3 4D 2.5	29 190.91	p5f3d 4D4Fe 3.5	271 108.5
413.458	43	5.36E+10	−0.71	413.456	0.004	0.002	p6f3 2L 7.5	31 036.00	p5f3d 2I2Kd 6.5	272 899.7
413.557	36	7.17E+10	−0.54	413.5475	0.0023	0.009	p6f3 4I 7.5	5988.51	p5f3s 4I4Kb 6.5	247 798.7
413.640	57	5.86E+11	0.79	413.640	0.005	0.000	p6f3 4I 7.5	5988.51	p5f3d 4I4Hc 6.5	247 744.4
413.770blV	39	7.38E+09	0.06	413.773	0.004	−0.003	p6f3 4I 5.5	1897.11	p5f3d 2I4Hb 6.5	243 575.6
413.878	65	1.49E+11	−0.60	413.881	0.004	−0.003	p6f3 4G 4.5	19 969.79	p5f3d 4G4Ge 3.5	261 585.0
413.925	61	5.06E+11	−0.58	413.924	0.004	0.001	p6f3 2L 7.5	31 036.00	p5f3d 2L2Le 8.5	272 626.1
414.052	57	6.30E+11	−0.87	414.049	0.003	0.004	p6f3 2K 6.5	20 005.22	p5f3d 2K2Ke 6.5	261 522.8
414.125	87	1.13E+12	0.92	414.115	0.004	0.011	p6f3 2L 7.5	31 036.00	p5f3d 2L2Me 8.5	272 514.9
414.225	41	2.50E+10	−0.26	414.221	0.003	0.004	p6f3 2G2 4.5	21 493.39	p5f3d 4G4Ge 5.5	262 910.4
414.324	83	1.23E+12	−0.90	414.326	0.004	−0.003	p6f3 2I 6.5	31 582.85	p5f3d 2I2Kd 7.5	272 938.4
414.496	56	5.49E+11	0.87	414.486	0.004	0.010	p6f3 4D 3.5	31 355.04	p5f3d 4D4Df 3.5	272 617.7
414.565	100	4.55E+11	−0.84	414.565	0.005	0.000	p6f3 2I 5.5	30 179.93	p5f3d 2I2Ie 5.5	271 396.5
414.641	63	2.03E+10	−0.28	414.648	0.004	−0.007	p6f3 4G 5.5	22 047.39	p5f3d 2K2If 5.5	263 215.7
414.835	81	9.89E+11	−0.88	414.835	0.005	0.000	p6f3 4G 5.5	22 047.39	p5f3d 4G4Hd 6.5	263 107.0
414.992	112	1.79E+12	−0.90	414.992	0.005	0.000	p6f3 2L 8.5	32 563.57	p5f3d 2L2Md$_b$ 9.5	273 532.0
415.074	50	4.57E+10	0.21	415.059	0.003	0.014	p6f3 4G 3.5	19 540.80	p5f3d 2G4H2 4.5	260 470.3
415.113	110	1.42E+11	0.58	415.112	0.003	0.002	p6f3 4I 5.5	1897.11	p5f3d 2L2Ka 6.5	242 796.2
415.172	97	7.25E+11	−0.84	415.174	0.003	−0.001	p6f3 4G 5.5	22 047.39	p5f3d 4G4Ge 5.5	262 910.4
415.276	65	1.40E+12	−0.95	415.276	0.005	0.000	p6f3 2K 6.5	20 005.22	p5f3d 2K2Ld 7.5	260 809.0
415.339	77	2.06E+11	0.63	415.337	0.004	0.002	p6f3 2H2 4.5	12 800.29	p5f3d 2F4I1 5.5	253 568.5
415.435	83	4.86E+11	−0.83	415.429	0.003	0.005	p6f3 4F 3.5	13 719.82	p5f3d 4F4Gd 4.5	254 434.6
415.561	117	4.11E+11	0.91	415.563	0.003	−0.002	p6f3 4I 5.5	1897.11	p5f3d 4I4If 5.5	242 534.5
415.750	43	3.15E+11	−0.91	415.750	0.005	−0.001	p6f3 2D1 2.5	24 333.10	p5f3d 2D2F1 3.5	264 862.0
415.836	34	1.18E+11	0.35	415.842	0.004	−0.006	p6f3 4I 6.5	3907.43	p5f3d 2I2Kc$_b$ 7.5	244 383.4
416.020	43	9.69E+10	0.71	416.017	0.004	0.003	p6f3 2L 8.5	32 563.57	p5f3d 2I2Kd 7.5	272 938.4
416.088	89	1.50E+12	−0.88	416.088	0.005	0.000	p6f3 2K 7.5	22 043.77	p5f3d 2K2Ld 8.5	262 377.5
416.393	101	9.73E+11	−0.91	416.392	0.004	0.001	p6f3 2L 7.5	31 036.00	p5f3d 2L2Le 7.5	271 194.2
416.557	69	1.17E+12	−0.88	416.558	0.004	−0.001	p6f3 2L 8.5	32 563.57	p5f3d 2L2Le 8.5	272 626.1
416.656	79	1.44E+12	−0.89	416.656	0.005	0.001	p6f3 2K 7.5	22 043.77	p5f3d 2K2Ke 7.5	262 050.0

(*continued on next page*)

Table 1 (*continued*)

λ_{exp}(Å)	Int_{exp}	$gA(s^{-1})$	CF	λ_{Ritz}(Å)	$\delta\lambda_{Ritz}$(Å)	$\Delta\lambda$(Å)	Lower level label	E_{low}	Upper level label	E_{up}
416.741bl	51	5.17E+11	−0.61	416.751	0.004	−0.010	p6f3 2L 8.5	32 563.57	p5f3d 2L2Me 8.5	272 514.9
417.093	31	1.66E+10	−0.07	417.095	0.004	−0.002	p6f3 4D 3.5	31 355.04	p5f3d 4D4Fe 3.5	271 108.5
417.165	66	7.42E+11	−0.82	417.160	0.003	0.005	p6f3 4I 7.5	5988.51	p5f3d 4I4Kd 8.5	245 704.8
417.246	80	1.97E+11	0.69	417.244	0.004	0.002	p6f3 4I 6.5	3907.43	p5f3d 2I4Hb 6.5	243 575.6
417.641	74	4.28E+10	−0.41	417.642	0.003	0.000	p6f3 4F 4.5	14 994.87	p5f3d 4F4Gd 4.5	254 434.6
417.759	57	5.13E+10	0.62	417.7874	0.0019	−0.028	p6f3 4I 4.5	0.00	p5f3d(s) 4G4Ha 4.5	239 356.2
417.849	87	5.09E+11	0.82	417.858	0.004	−0.009	p6f3 4I 5.5	1897.11	p5f3d 4I4Ka 6.5	241 212.6
418.188	62	1.86E+09	−0.03	418.192	0.004	−0.004	p6f3 4I 6.5	3907.43	p5f3d 2I2Kc 7.5	243 032.1
418.608	64	4.59E+10	0.53	418.605	0.003	0.004	p6f3 4I 6.5	3907.43	p5f3d 2L2Ka 6.5	242 796.2
418.805	65	6.15E+10	0.50	418.802	0.004	0.003	p6f3 2H1 5.5	35 136.61	p5f3d 2I2Ie 6.6	273 912.9
418.925bl	82	7.96E+09	−0.42	418.920	0.003	0.004	p6f3 4I 4.5	0.00	p5f3d 2G2H2 5.5	238 709.0
419.024	34	1.97E+10	0.38	419.030	0.003	−0.006	p6f3 2H1 4.5	33 741.15	p5f3d 2I2Hf 4.5	272 387.5
419.156bl	59	1.67E+10	0.07	419.158	0.004	−0.002	p6f3 4F 4.5	14 994.87	p5f3d 2F4I1 5.6	253 568.5
419.214	27	5.97E+10	0.27	419.213	0.004	0.001	p6f3 2H1 5.5	35 136.61	p5f3d 2I2Hf 5.5	273 678.6
419.478	94	4.44E+11	0.91	419.472	0.004	0.006	p6f3 4I 7.5	5988.51	p5f3d 2I2Kc$_b$ 7.5	244 383.4
419.682	21	1.13E+10	0.34	419.687	0.003	−0.005	p6f3 2H2 5.5	16 161.53	p5f3d 4F4Gd 4.5	254 434.6
419.919	44	3.85E+10	−0.59	419.9153	0.0024	0.004	p6f3 4I 5.5	1897.11	p5f3d 2I2Ke 6.5	240 040.4
421.124	20	6.57E+09	0.36	421.1252	0.0020	−0.001	p6f3 4I 5.5	1897.11	p5f3d(s) 4G4Ha 4.5	239 356.2
421.179	13	1.23E+10	−0.34	421.1754	0.0019	0.004	p6f3 4I 5.5	1897.11	p5f3d 2L4L 6.5	239 327.9
421.407	19	7.45E+09	−0.04	421.398	0.004	0.009	p6f3 4I 6.5	3907.43	p5f3d 4I4Ka 6.5	241 212.6
421.496	31	1.26E+10	0.04	421.495	0.003	0.001	p6f3 2H1 5.5	35 136.61	p5f3d 2I2Hf 4.5	272 387.5
421.867	23	7.23E+10	−0.79	421.863	0.004	0.004	p6f3 4I 7.5	5988.51	p5f3d 2I2Kc 7.5	243 032.1
422.275	22	3.65E+10	0.60	422.276	0.003	−0.001	p6f3 4I 5.5	1897.11	p5f3d 2G2H2 5.5	238 709.0
422.361	25	6.69E+10	−0.78	422.363	0.003	−0.002	p6f3 4I 6.5	3907.43	p5f3d 2G4I2$_b$ 7.5	240 670.5
423.199	95	2.07E+11	0.81	423.2075	0.0025	−0.009	p6f3 4I 7.5	5988.51	p5f3d 2L4Ka 8.5	242 279.2
423.783	48	5.67E+09	−0.18	423.7891	0.0021	−0.006	p6f3 4I 4.5	0.00	p5f3d 2K4Hb 5.5	235 966.4
423.951	23	3.50E+10	0.67	423.9611	0.0022	−0.011	p6f3 4I 6.5	3907.43	p5f3d 2G4I2 7.5	239 778.1
424.760	10	2.25E+10	0.46	424.7719	0.0019	−0.011	p6f3 4I 6.5	3907.43	p5f3d 2L4L 6.5	239 327.9
427.448	25	1.35E+10	0.47	427.4429	0.0021	0.005	p6f3 4I 6.5	3907.43	p5f3d 2I4K 6.5	237 856.8
427.733	45	5.78E+09	0.29	427.735	0.002	−0.002	p6f3 4I 7.5	5988.51	p5f3d 2G4I2 7.5	239 778.1
427.941bl	32	8.52E+09	−0.27	427.940	0.003	0.001	p6f3 4I 7.5	5988.51	p5f3d 2K2Mc 8.5	239 666.0
428.710	39	1.51E+10	0.54	428.7075	0.0025	0.003	p6f3 4I 5.5	1897.11	p5f3d 2I4K 5.5	235 156.4
430.221	11	8.79E+09	0.46	430.215	0.003	0.006	p6f3 4I 7.5	5988.51	p5f3d 4G4Hb 6.5	238 430.3
430.916	13	2.10E+09	−0.25	430.9249	0.0022	−0.009	p6f3 4I 6.5	3907.43	p5f3d 2K4Hb 5.5	235 966.4
430.965	24	1.88E+07	0.00	430.9632	0.0022	0.002	p6f3 4I 4.5	0.00	p5f3d 2G4G1 5.5	232 038.4
431.594	39	1.52E+10	0.43	431.609	0.003	−0.015	p6f3 4I 7.5	5988.51	p5f3d 2K4Ka 8.5	237 679.7
433.820	29	5.79E+09	−0.33	433.822	0.003	−0.003	p6f3 4I 5.5	1897.11	p5f3d 4G4Hc 6.5	232 406.2
434.919	12	3.87E+09	−0.39	434.928	0.003	−0.008	p6f3 4I 6.5	3907.43	p5f3d 4G4Hc$_b$ 6.5	233 830.6
438.348	11	2.16E+09	−0.17	438.3447	0.0023	0.004	p6f3 4I 6.5	3907.43	p5f3d 2G4G1 5.5	232 038.4
438.820	31	2.62E+09	0.16	438.8158	0.0022	0.004	p6f3 4I 6.5	3907.43	p5f3d 2G2K2 7.5	231 793.5
438.913	33	3.04E+09	0.32	438.900	0.003	0.012	p6f3 4I 7.5	5988.51	p5f3d 4G4Hc$_b$ 6.5	233 830.6
438.988	38	7.06E+09	−0.25	438.994	0.003	−0.006	p6f3 2K 6.5	20 005.22	p5f3s 4I4Kb 6.5	247 798.7
439.554	32	1.11E+09	−0.08	439.5597	0.0019	−0.006	p6f3 4I 5.5	1897.11	p5f3d 2K4Hb 6.5	229 397.5
440.129blV	20	2.08E+09	−0.09	440.115	0.003	0.014	p6f3 4I 6.5	3907.43	p5f3d 2L4M 7.5	231 120.8
440.584	26	2.66E+08	−0.01	440.5676	0.0021	0.016	p6f3 4F 4.5	14 994.87	p5f3d 2I4Gb 4.5	241 974.8
440.861	47	3.73E+08	0.06	440.8472	0.0025	0.014	p6f3 4I 7.5	5988.51	p5f3d 2G2K2 6.5	232 824.5
441.311	29	4.62E+09	−0.06	441.3131	0.0023	−0.002	p6f3 2H2 5.5	16 161.53	p5f3d 4D4Ga 5.5	242 758.0
441.679blV	42	1.38E+10	−0.57	441.682	0.003	−0.002	p6f3 4I 7.5	5988.51	p5f3d 4G4Ka 8.5	232 396.0
441.714blV	46	1.90E+10	−0.17	441.723	0.003	−0.009	p6f3 2H1 5.5	35 136.61	p5f3d 2K2Ke 6.5	261 522.8
442.772	16	2.80E+09	−0.16	442.758	0.003	0.014	p6f3 4I 7.5	5988.51	p5f3d 2K2Ma 8.5	231 845.6
442.878blV	21	3.34E+09	0.11	442.8600	0.0022	0.018	p6f3 4I 7.5	5988.51	p5f3d 2G2K2 7.5	231 793.5
442.961	26	1.12E+10	−0.28	442.965	0.003	−0.005	p6f3 4G 5.5	22 047.39	p5f3s 4I4Kb 6.5	247 798.7
444.192	4	4.68E+09	−0.29	444.183	0.003	0.008	p6f3 4I 7.5	5988.51	p5f3d 2L4M 7.5	231 120.8
445.718	22	1.14E+09	0.03	445.7096	0.0022	0.008	p6f3 4F 4.5	14 994.87	p5f3d(s) 4G4Ha 4.5	239 356.2
446.797	13	8.39E+08	0.10	446.7932	0.0017	0.004	p6f3 4I 6.5	3907.43	p5f3d 2L2Ha 5.5	227 724.6
447.311	28	3.33E+09	−0.10	447.3171	0.0019	−0.006	p6f3 4I 6.5	3907.43	p5f3d 2L4H 6.5	227 462.5
448.076	45	3.05E+09	0.06	448.0918	0.0021	−0.016	p6f3 4I 6.5	3907.43	p5f3d 4I2Ia 6.5	227 076.0
448.943p	47	3.80E+08	0.03	448.9282	0.0024	0.015	p6f3 2K 6.5	20 005.22	p5f3d 4D4Ga 5.5	242 758.0
449.340	68	6.66E+09	−0.07	449.342	0.003	−0.003	p6f3 2H2 5.5	16 161.53	p5f3d 2G2H2 5.5	238 709.0
450.400	65	3.02E+09	0.15	450.4138	0.0017	−0.014	p6f3 4I 6.5	3907.43	p5f3d 2H2I1 6.5	225 925.5
452.406blV	61	3.13E+09	−0.08	452.405	0.004	0.001	p6f3 2G2 4.5	21 493.39	p5f3d 4I4If 5.5	242 534.5
452.991blV	30	2.20E+09	−0.02	452.996	0.003	−0.005	p6f3 2K 7.5	22 043.77	p5f3d 2L2Ka 6.5	242 796.2
453.176blV	84	2.91E+09	0.15	453.175	0.003	0.001	p6f3 2K 6.5	20 005.22	p5f3d 2G4I2$_b$ 7.5	240 670.5
453.747	42	3.16E+09	0.15	453.760	0.003	−0.013	p6f3 4I 6.5	3907.43	p5f3d 2H4K1 7.5	224 288.2
453.829	37	3.25E+08	0.00	453.831	0.003	−0.003	p6f3 4I 6.5	3907.43	p5f3d(s) 4F6G 6.5	224 253.6
454.212	19	3.94E+09	0.15	454.2265	0.0017	−0.015	p6f3 4I 6.5	3907.43	p5f3d 2H2I1 5.5	224 061.9
454.925	54	7.62E+09	0.10	454.9272	0.0023	−0.002	p6f3 4G 3.5	19 540.80	p5f3d(s) 4G4Ha 4.5	239 356.2
455.029	26	4.76E+09	−0.16	455.015	0.003	0.014	p6f3 2K 6.5	20 005.22	p5f3d 2G4I2 7.5	239 778.1
455.954blV	18	1.88E+09	−0.06	455.9492	0.0022	0.005	p6f3 2K 6.5	20 005.22	p5f3d 2L4L 6.5	239 327.9
456.123	73	2.50E+09	0.03	456.1251	0.0025	−0.003	p6f3 2H2 4.5	12 800.29	p5f3d 2G4G1 5.5	232 038.4
457.126	32	4.16E+08	0.01	457.130	0.003	−0.004	p6f3 4I 6.5	3907.43	p5f3d 2D4H2 5.5	222 663.7
457.822	105	6.14E+09	0.19	457.823	0.003	−0.001	p6f3 2K 6.5	20 005.22	p5f3d 4G4Hb 6.5	238 430.3
458.099blV	29	6.25E+09	0.18	458.086	0.003	0.014	p6f3 4I 7.5	5988.51	p5f3d 2H4K1 7.5	224 288.2
458.162	51	1.02E+05	0.00	458.158	0.003	0.003	p6f3 4I 7.5	5988.51	p5f3d(s) 4F6G 6.5	224 253.6
459.033	12	3.99E+09	−0.05	459.0281	0.0024	0.004	p6f3 2K 6.5	20 005.22	p5f3d 2I4K 6.5	237 856.8

(*continued on next page*)

Table 1 (*continued*)

λ_{exp}(Å)	Int_{exp}	$gA(s^{-1})$	CF	λ_{Ritz}(Å)	$\delta\lambda_{Ritz}$(Å)	$\Delta\lambda$(Å)	Lower level label	E_{low}	Upper level label	E_{up}
459.410	109	1.59E+10	−0.12	459.413	0.003	−0.003	p6f3 2H2 5.5	16 161.53	p5f3d 4G4Hc$_b$ 6.5	233 830.6
459.507	135	2.28E+10	−0.07	459.512	0.003	−0.005	p6f3 2K 7.5	22 043.77	p5f3d 2K2Mc 8.5	239 666.0
463.749	28	2.58E+09	0.01	463.745	0.003	0.005	p6f3 2K 7.5	22 043.77	p5f3d 2K4Ka 8.5	237 679.7
464.724	32	5.80E+09	0.11	464.713	0.003	0.012	p6f3 4G 4.5	19 969.79	p5f3d 2I4K 5.5	235 156.4
465.239	21	9.63E+09	0.05	465.236	0.003	0.003	p6f3 4I 7.5	5988.51	p5f3d 4I4Ka 8.5	220 933.1
465.830	13	1.29E+10	−0.06	465.834	0.004	−0.004	p6f3 2L 7.5	31 036.00	p5f3d 4I4Kd 8.5	245 704.8
466.256	27	4.09E+09	0.09	466.259	0.003	−0.003	p6f3 2G2 4.5	21 493.39	p5f3d 2K4Hb 5.5	235 966.4
466.976blV	27	1.03E+09	−0.01	466.980	0.004	−0.004	p6f3 2H2 4.5	12 800.29	p5f3d 4F4Gc 4.5	226 942.2
468.851	39	1.41E+09	0.01	468.848	0.003	0.003	p6f3 2K 7.5	22 043.77	p5f3d 2L4Na 8.5	235 332.7
470.071blV	25	1.50E+08	0.00	470.0800	0.0019	−0.009	p6f3 4F 4.5	14 994.87	p5f3d 2L2Ha 5.5	227 724.6
470.810	49	1.58E+09	0.06	470.808	0.003	0.002	p6f3 2K 6.5	20 005.22	p5f3d 4G4Hc 6.5	232 406.2
471.439	30	5.37E+09	−0.12	471.436	0.003	0.003	p6f3 4I 6.5	3907.43	p5f3d 2K4L 6.5	216 025.3
471.819	39	1.19E+09	−0.02	471.815	0.004	0.003	p6f3 4F 4.5	14 994.87	p5f3d 4F4Gc 4.5	226 942.2
472.133	61	1.01E+10	0.15	472.1550	0.0024	−0.022	p6f3 2I 5.5	30 179.93	p5f3d 2I4Gb 4.5	241 974.8
472.747a	46	7.87E+09	−0.17	472.729	0.004	0.018	p6f3 4I 5.5	1897.11	p5f3d 4I4Kb 6.5	213 434.6
473.256	14	4.73E+08	0.01	473.2586	0.0021	−0.002	p6f3 2H2 5.5	16 161.53	p5f3d 2L4H 6.5	227 462.5
473.387blV	37	6.94E+09	−0.06	473.388	0.003	−0.001	p6f3 2L 7.5	31 036.00	p5f3d 2L4Ka 8.5	242 279.2
473.548	25	4.46E+08	0.01	473.541	0.003	0.007	p6f3 2I 6.5	31 582.85	p5f3d 4D4Ga 5.5	242 758.0
474.111blV	34	5.88E+09	−0.09	474.1258	0.0024	−0.015	p6f3 2H2 5.5	16 161.53	p5f3d 4I2Ia 6.5	227 076.0
475.147	15	4.68E+08	0.00	475.147	0.003	−0.001	p6f3 2K 7.5	22 043.77	p5f3d 2G2K1 7.5	232 504.8
475.378	30	2.15E+09	−0.02	475.378	0.003	0.000	p6f3 4G 5.5	22 047.39	p5f3d 4G4Hc 6.5	232 406.2
476.628	75	1.18E+10	−0.17	476.640	0.004	−0.012	p6f3 2K 7.5	22 043.77	p5f3d 2K2Ma 8.5	231 845.6
476.845	50	9.14E+09	0.19	476.836	0.003	0.009	p6f3 2L 8.5	32 563.57	p5f3d 2L4Ka 8.5	242 279.2
477.248	23	1.41E+09	0.05	477.265	0.004	−0.017	p6f3 4I 6.5	3907.43	p5f3d 4I4Kb 6.5	213 434.6
477.569	19	1.71E+08	0.01	477.5725	0.0022	−0.003	p6f3 2K 6.5	20 005.22	p5f3d 2K4Hb 6.5	229 397.5
478.299	80	1.33E+09	0.02	478.3155	0.0018	−0.017	p6f3 4F 4.5	14 994.87	p5f3d 2H2I1 5.5	224 061.9
478.449	67	6.36E+09	−0.11	478.459	0.003	−0.010	p6f3 2L 7.5	31 036.00	p5f3d 2I2Ke 6.5	240 040.4
478.813	7	6.44E+08	0.00	478.810	0.004	0.003	p6f3 2K 7.5	22 043.77	p5f3d 2L2Md 8.5	230 894.7
479.321	31	9.77E+07	0.00	479.317	0.003	0.003	p6f3 2L 7.5	31 036.00	p5f3d 2K2Mc 8.5	239 666.0
480.104	90	1.86E+10	0.30	480.0955	0.0025	0.008	p6f3 2L 7.5	31 036.00	p5f3d 2L4L 6.5	239 327.9
480.236	10	3.78E+09	0.05	480.2298	0.0024	0.006	p6f3 2H1 4.5	33 741.15	p5f3d 2I4Gb 4.5	241 974.8
480.522	50	3.67E+09	−0.05	480.522	0.003	0.000	p6f3 2L 8.5	32 563.57	p5f3d 2G4I2$_b$ 7.5	240 670.5
481.435blV	67	1.08E+10	−0.30	481.4187	0.0020	0.016	p6f3 2K 6.5	20 005.22	p5f3d 2L2Ha 5.5	227 724.6
481.509blV	37	8.66E+09	0.14	481.517	0.003	−0.008	p6f3 2I 5.5	30 179.93	p5f3d 2I4K 6.5	237 856.8
481.628	50	1.75E+09	0.02	481.646	0.003	−0.018	p6f3 2H1 5.5	35 136.61	p5f3d 4D4Ga 5.5	242 758.0
482.274	72	1.16E+10	0.23	482.2677	0.0022	0.006	p6f3 2K 7.5	22 043.77	p5f3d 2K4Hb 6.5	229 397.5
482.588	36	4.14E+09	0.05	482.592	0.003	−0.003	p6f3 2L 8.5	32 563.57	p5f3d 2G4I2 7.5	239 778.1
483.190	62	3.32E+10	−0.61	483.190	0.005	0.000	p6f3 2L 8.5	32 563.57	p5f3d 2L4Na 9.5	239 521.7
483.474blV	35	1.59E+09	−0.03	483.4697	0.0025	0.004	p6f3 2H1 5.5	35 136.61	p5f3d 2I4Gb 4.5	241 974.8
484.188	53	1.84E+10	−0.14	484.188	0.005	0.000	p6f3 2L 8.5	32 563.57	p5f3d 2K2Kd 7.5	239 094.8
484.244blV	57	1.17E+10	0.14	484.237	0.003	0.007	p6f3 2K 7.5	22 043.77	p5f3d 2L2Lf 8.5	228 554.3
484.793	43	6.84E+09	−0.12	484.792	0.003	0.000	p6f3 2I 6.5	31 582.85	p5f3d 2I4K 6.5	237 856.8
486.187	14	1.11E+09	−0.04	486.1987	0.0020	−0.012	p6f3 4G 5.5	22 047.39	p5f3d 2L2Ha 5.5	227 724.6
486.677	56	8.15E+09	−0.05	486.695	0.004	−0.018	p6f3 2L 7.5	31 036.00	p5f3d 2L4Mb 8.5	236 503.5
486.818	18	2.77E+09	0.12	486.8191	0.0022	−0.001	p6f3 4G 5.5	22 047.39	p5f3d 2L4H 6.5	227 462.5
487.536	87	1.41E+10	−0.14	487.529	0.003	0.008	p6f3 2L 8.5	32 563.57	p5f3d 2K4Ka 8.5	237 679.7
487.739	28	2.29E+09	−0.16	487.728	0.003	0.011	p6f3 2K 7.5	22 043.77	p5f3d 4I2Ia 6.5	227 076.0
487.849	30	3.18E+09	−0.09	487.861	0.003	−0.012	p6f3 2I 5.5	30 179.93	p5f3d 2I4K 5.5	235 156.4
487.934	44	9.98E+09	−0.15	487.938	0.003	−0.004	p6f3 2K 6.5	20 005.22	p5f3d 2H2L1 7.5	224 949.2
488.040	17	3.91E+09	−0.03	488.034	0.003	0.006	p6f3 2H1 5.5	35 136.61	p5f3d 2I2Ke 6.5	240 040.4
489.480p	134	3.07E+10	−0.22	489.484	0.003	−0.005	p6f3 2L 7.5	31 036.00	p5f3d 2L4Na 8.5	235 332.7
489.685	29	1.09E+09	0.05	489.669	0.003	0.016	p6f3 2H1 5.5	35 136.61	p5f3d(s) 4G4Ha 4.5	239 356.2
489.730	20	2.50E+09	−0.04	489.737	0.003	−0.007	p6f3 2H1 5.5	35 136.61	p5f3d 2L4L 6.5	239 327.9
489.996	12	6.53E+08	0.02	489.975	0.0019	0.021	p6f3 4G 4.5	19 969.79	p5f3d 2H2I1 5.5	224 061.9
490.068	17	5.50E+09	0.31	490.0600	0.0019	0.008	p6f3 2K 6.5	20 005.22	p5f3d 2H2I1 5.5	224 061.9
490.358	59	9.49E+09	0.06	490.340	0.004	0.018	p6f3 2L 8.5	32 563.57	p5f3d 2L4Mb 8.5	236 503.5
490.484	65	1.39E+10	0.21	490.4804	0.0020	0.003	p6f3 2K 7.5	22 043.77	p5f3d 2H2I1 6.5	225 925.5
491.895bl	24	4.37E+09	0.06	491.899	0.003	−0.004	p6f3 2H1 5.5	35 136.61	p5f3d 4G4Hb 6.5	238 430.3
492.830blV	67	3.77E+09	−0.10	492.840	0.003	−0.010	p6f3 2K 7.5	22 043.77	p5f3d 2H2L1 7.5	224 949.2
493.053	68	9.52E+09	−0.39	493.052	0.005	0.000	p6f3 4I 7.5	5988.51	p5f3d 4I4La 7.5	208 806.7
493.173	16	5.57E+09	−0.12	493.172	0.003	0.001	p6f3 2L 8.5	32 563.57	p5f3d 2L4Na 8.5	235 332.7
493.471	42	1.50E+10	−0.27	493.475	0.003	−0.004	p6f3 2I 5.5	30 179.93	p5f3d 2G2K2 6.5	232 824.5
494.450as	88	1.90E+10	0.39	494.451	0.003	−0.001	p6f3 2K 7.5	22 043.77	p5f3d 2H4K1 7.5	224 288.2
494.544	28	4.97E+09	0.13	494.545	0.003	−0.001	p6f3 4G 5.5	22 047.39	p5f3d(s) 4F6G 6.5	224 253.6
494.973as	63	4.02E+10	−0.20	494.973	0.005	0.000	p6f3 2L 8.5	32 563.57	p5f3d 2L2Md 9.5	234 594.7
495.561	14	2.49E+09	0.19	495.568	0.003	−0.007	p6f3 2L 7.5	31 036.00	p5f3d 2G2K2 6.5	232 824.5
496.355blV	36	1.03E+09	0.02	496.355	0.004	0.001	p6f3 2L 7.5	31 036.00	p5f3d 2G2K1 7.5	232 504.8
497.095	87	9.75E+09	0.35	497.091	0.004	0.003	p6f3 2G2 4.5	21 493.39	p5f3d 2D4H2 5.5	222 663.7
497.947	36	1.72E+09	−0.05	497.934	0.003	0.013	p6f3 2H1 5.5	35 136.61	p5f3d 2K4Hb 5.5	235 966.4
498.098blV	26	7.05E+09	−0.23	498.113	0.003	−0.015	p6f3 2L 7.5	31 036.00	p5f3d 2G2K2 7.5	231 793.5
498.862	25	1.91E+09	0.14	498.864	0.003	−0.002	p6f3 2I 6.5	31 582.85	p5f3d 2G4G1 5.5	232 038.4
499.384	73	1.54E+10	0.48	499.384	0.005	0.000	p6f3 4I 7.5	5988.51	p5f3d 2L4L 8.5	206 235.2
499.471	35	6.43E+09	−0.18	499.474	0.003	−0.002	p6f3 2I 6.5	31 582.85	p5f3d 2G2K2 7.5	231 793.5
499.771	73	2.76E+10	−0.37	499.788	0.003	−0.018	p6f3 2L 7.5	31 036.00	p5f3d 2L4M 7.5	231 120.8
500.348D	84	1.66E+10	0.43	500.358	0.004	−0.009	p6f3 4I 7.5	5988.51	p5f3d 4G4Kb 8.5	205 845.6

(*continued on next page*)

Table 1 (*continued*)

λ_{exp}(Å)	Int_{exp}	$gA(s^{-1})$	CF	λ_{Ritz}(Å)	$\delta\lambda_{Ritz}$(Å)	$\Delta\lambda$(Å)	Lower level label	E_{low}	Upper level label	E_{up}
500.348D	84	1.92E+10	−0.08	500.353	0.004	−0.005	p6f3 2L 7.5	31 036.00	p5f3d 2L2Md 8.5	230 894.7
500.421blV	43	1.07E+10	0.18	500.419	0.004	0.002	p6f3 2L 8.5	32 563.57	p5f3d 4G4Ka 8.5	232 396.0
500.557	23	1.94E+07	0.00	500.5576	0.0023	−0.001	p6f3 4I 5.5	1897.11	p5f3d 4G4Ka 6.5	201 674.3
500.693	12	3.13E+09	0.10	500.690	0.004	0.002	p6f3 4I 5.5	1897.11	p5f3d 4F4Gd 5.5	201 621.4
501.213	67	8.36E+09	0.14	501.213	0.005	0.000	p6f3 2K 7.5	22 043.77	p5f3d 4I4Ka$_b$ 8.5	221 559.6
501.968	8	1.10E+09	0.03	501.9638	0.0024	0.005	p6f3 2I 5.5	30 179.93	p5f3d 2K4Hb 6.5	229 397.5
502.801	36	1.16E+10	0.20	502.792	0.003	0.009	p6f3 2K 7.5	22 043.77	p5f3d 4I4Ka 8.5	220 933.1
504.350	7	8.85E+08	−0.06	504.347	0.002	0.003	p6f3 4I 5.5	1897.11	p5f3d 4G6Gb 6.5	200 173.3
505.521	17	2.30E+09	0.11	505.5237	0.0025	−0.003	p6f3 2I 6.5	31 582.85	p5f3d 2K4Hb 6.5	229 397.5
505.649	29	9.05E+09	−0.33	505.6459	0.0024	0.003	p6f3 4I 6.5	3907.43	p5f3d 4G4Ka 6.5	201 674.3
505.779	39	5.14E+09	0.20	505.781	0.004	−0.002	p6f3 4I 6.5	3907.43	p5f3d 4F4Gd 5.5	201 621.4
506.149	33	1.22E+10	0.38	506.141	0.004	0.007	p6f3 4I 6.5	3907.43	p5f3d 4F6Hb 7.5	201 480.7
509.091	11	5.22E+08	0.02	509.0963	0.0024	−0.005	p6f3 2L 7.5	31 036.00	p5f3d 2L4H 6.5	227 462.5
509.504	29	1.46E+08	0.00	509.5129	0.0020	−0.009	p6f3 4I 6.5	3907.43	p5f3d 4G6Gb 6.5	200 173.3
510.150bl	12	8.74E+09	−0.40	510.152	0.004	−0.002	p6f3 2K 6.5	20 005.22	p5f3d 2K4L 6.5	216 025.3
510.222	21	1.49E+10	0.12	510.228	0.004	−0.006	p6f3 2L 8.5	32 563.57	p5f3d 2L2Lf 8.5	228 554.3
510.478	33	6.51E+08	−0.05	510.490	0.003	−0.012	p6f3 4I 4.5	0.00	p5f3d 2H2H2 5.5	195 890.1
510.531	59	2.98E+09	−0.14	510.5176	0.0025	0.013	p6f3 2I 6.5	31 582.85	p5f3d 2L4H 6.5	227 462.5
510.877	10	2.69E+09	−0.06	510.867	0.002	0.010	p6f3 2I 5.5	30 179.93	p5f3d 2H2I1 6.5	225 925.5
511.019	13	1.62E+09	−0.18	511.0233	0.0024	−0.005	p6f3 4I 7.5	5988.51	p5f3d 4G4Ka 6.5	201 674.3
511.522	8	7.51E+08	0.02	511.529	0.004	−0.007	p6f3 4I 7.5	5988.51	p5f3d 4F6Hb 7.5	201 480.7
513.327	42	5.27E+09	0.20	513.325	0.003	0.002	p6f3 4I 5.5	1897.11	p5f3d 4G6G 6.5	196 705.6
514.553	52	3.86E+09	−0.18	514.5550	0.0022	−0.003	p6f3 2I 6.5	31 582.85	p5f3d 2H2I1 6.5	225 925.5
514.976	26	9.28E+09	0.17	514.9734	0.0021	0.002	p6f3 4I 7.5	5988.51	p5f3d 4G6Gb 6.5	200 173.3
515.505	35	1.61E+09	0.04	515.5079	0.0023	−0.003	p6f3 2H1 4.5	33 741.15	p5f3d 2L2Ha 5.5	227 724.6
517.166	23	1.04E+09	−0.01	517.153	0.003	0.013	p6f3 2I 6.5	31 582.85	p5f3d 2H2L1 7.5	224 949.2
519.247	19	1.66E+09	−0.06	519.2432	0.0023	0.004	p6f3 2H1 5.5	35 136.61	p5f3d 2L2Ha 5.5	227 724.6
519.375	59	4.59E+09	0.11	519.3680	0.0019	0.007	p6f3 4I 4.5	0.00	p5f3d 4I6Lb$_b$ 5.5	192 541.7
519.577	39	1.40E+09	−0.04	519.5770	0.0022	0.000	p6f3 4I 4.5	0.00	p5f3d 4I4Gd 5.5	192 464.3
520.894	15	2.00E+09	−0.10	520.888	0.003	0.006	p6f3 4I 5.5	1897.11	p5f3d 2H4H2 5.5	193 876.8
521.012	9	6.19E+08	0.01	520.998	0.003	0.014	p6f3 2H1 5.5	35 136.61	p5f3d 4I2Ia 6.5	227 076.0
521.667	54	2.81E+09	0.12	521.675	0.003	−0.008	p6f3 4I 4.5	0.00	p5f3d 4I6Lb 5.5	191 690.1
522.309	25	2.81E+08	0.05	522.324	0.003	−0.015	p6f3 4I 5.5	1897.11	p5f3d 2K4La 6.5	193 349.2
524.343	3	6.86E+08	0.01	524.337	0.003	0.006	p6f3 4I 7.5	5988.51	p5f3d 4G6G 6.5	196 705.6
524.519	5	2.37E+08	0.00	524.5363	0.0020	−0.017	p6f3 4I 5.5	1897.11	p5f3d 4I6Lb$_b$ 5.5	192 541.7
525.028	22	2.57E+08	−0.01	525.014	0.004	0.014	p6f3 4I 4.5	0.00	p5f3d 4G6Gb 5.5	190 471.1
526.341	53	2.20E+08	−0.03	526.328	0.003	0.013	p6f3 4I 4.5	0.00	p5f3d 4F6F 5.5	189 995.5
526.408	25	1.26E+09	−0.05	526.401	0.003	0.007	p6f3 4I 6.5	3907.43	p5f3d 2H4H2 5.5	193 876.8
526.591	5	2.32E+09	−0.04	526.601	0.003	−0.010	p6f3 2L 7.5	31 036.00	p5f3d 4I4Ka 8.5	220 933.1
527.869bl	37	2.92E+08	0.01	527.867	0.003	0.002	p6f3 4I 6.5	3907.43	p5f3d 2K4La 6.5	193 349.2
528.762	39	1.25E+09	0.07	528.762	0.005	0.000	p6f3 4I 6.5	3907.43	p5f3d 2H4L2 7.5	193 028.4
528.838	17	6.98E+07	0.00	528.8238	0.0025	0.014	p6f3 4I 4.5	0.00	p5f3d 2H4G2 3.5	189 098.9
530.113	12	1.40E+08	−0.01	530.1264	0.0020	−0.013	p6f3 4I 6.5	3907.43	p5f3d 4I6Lb$_b$ 5.5	192 541.7
530.282	16	8.25E+08	0.02	530.296	0.004	−0.013	p6f3 4I 5.5	1897.11	p5f3d 4G6Gb 5.5	190 471.1
532.053	21	8.41E+09	0.07	532.053	0.005	0.000	p6f3 2L 8.5	32 563.57	p5f3d 2L4Ma 9.5	220 514.9
532.551	12	8.61E+07	0.01	532.531	0.003	0.020	p6f3 4I 6.5	3907.43	p5f3d 4I6Lb 5.5	191 690.1
534.531	12	2.38E+09	0.17	534.531	0.005	0.000	p6f3 2L 8.5	32 563.57	p5f3d 4I2M 9.5	219 643.5
535.721	30	1.65E+09	0.03	535.717	0.003	0.004	p6f3 4I 5.5	1897.11	p5f3d 4F6I 5.5	188 563.0
538.158	52	9.57E+08	0.01	538.151	0.004	0.007	p6f3 4I 6.5	3907.43	p5f3d 4F6I 7.5	189 729.0
539.278	60	1.02E+09	−0.01	539.278	0.005	0.000	p6f3 4I 7.5	5988.51	p5f3d 4I4Lc 8.5	191 421.6
541.507	45	4.01E+07	0.00	541.500	0.002	0.007	p6f3 4I 6.5	3907.43	p5f3d 4G6Hb 5.5	188 579.7
544.068	5	2.38E+08	0.00	544.064	0.004	0.004	p6f3 2K 7.5	22 043.77	p5f3d 4G4Kb 8.5	205 845.6
544.698blV	6	7.14E+07	0.00	544.698	0.003	−0.001	p6f3 4I 4.5	0.00	p5f3d 4I2H 4.5	183 587.9
546.191	28	2.39E+08	0.00	546.180	0.004	0.010	p6f3 2H2 4.5	12 800.29	p5f3d 2H2H2 5.5	195 890.1
548.723	15	4.54E+07	0.00	548.725	0.003	−0.002	p6f3 4I 5.5	1897.11	p5f3d 4I6Ga$_b$ 6.5	184 137.8
549.839	34	1.84E+07	0.00	549.851	0.003	−0.012	p6f3 4I 5.5	1897.11	p5f3d 4F6Ha 6.5	183 764.4
550.399	28	4.45E+08	0.01	550.386	0.003	0.013	p6f3 4I 5.5	1897.11	p5f3d 4I2H 4.5	183 587.9
551.679	14	1.91E+08	0.00	551.676	0.003	0.002	p6f3 4I 5.5	1897.11	p5f3d 4I4Hf 6.5	183 162.8
553.425	29	4.98E+07	0.00	553.4169	0.0024	0.008	p6f3 4I 5.5	1897.11	p5f3d 4I6Ga 6.5	182 592.7
555.996	49	1.46E+08	0.00	555.997	0.003	−0.002	p6f3 4I 6.5	3907.43	p5f3d 4F6Ha 6.5	183 764.4
556.712	19	2.61E+08	−0.05	556.709	0.003	0.002	p6f3 4G 5.5	22 047.39	p5f3d 4G4Ka 6.5	201 674.3
559.623	29	3.02E+06	−0.00	559.6432	0.0024	−0.021	p6f3 4I 6.5	3907.43	p5f3d 4I6Ga 6.5	182 592.7
561.322	104	7.48E+08	−0.01	561.327	0.003	−0.004	p6f3 4I 7.5	5988.51	p5f3d 4I6Ga$_b$ 6.5	184 137.8
561.401	58	1.09E+09	0.04	561.4006	0.0024	0.001	p6f3 4G 5.5	22 047.39	p5f3d 4G6Gb 6.5	200 173.3
563.234	32	4.40E+07	0.00	563.2317	0.0023	0.002	p6f3 4F 4.5	14 994.87	p5f3d 4I6Lb$_b$ 5.5	192 541.7
564.414	72	1.18E+09	−0.01	564.416	0.004	−0.002	p6f3 4I 7.5	5988.51	p5f3d 4I4Hf 6.5	183 162.8
566.255	40	3.05E+08	0.00	566.238	0.003	0.017	p6f3 4I 7.5	5988.51	p5f3d 4I6Ga 6.5	182 592.7
571.416	96	1.39E+08	−0.01	571.427	0.004	−0.011	p6f3 4F 4.5	14 994.87	p5f3d 4F6F 5.5	189 995.5
572.540	36	4.58E+08	−0.03	572.547	0.003	−0.007	p6f3 4G 5.5	22 047.39	p5f3d 4G6G 6.5	196 705.6
574.881	43	1.85E+08	−0.01	574.8822	0.0023	−0.001	p6f3 2H2 5.5	16 161.53	p5f3d 4F6F 4.5	190 110.2
576.139	29	7.15E+07	−0.01	576.143	0.004	−0.004	p6f3 4F 4.5	14 994.87	p5f3d 4F6I 5.5	188 563.0
576.898	21	4.62E+07	−0.01	576.888	0.003	0.010	p6f3 2K 6.5	20 005.22	p5f3d 2K4La 6.5	193 349.2
579.990	37	1.10E+08	−0.01	579.985	0.003	0.005	p6f3 2H2 5.5	16 161.53	p5f3d 4G6Hb 5.5	188 579.7
581.962	39	3.93E+08	−0.02	581.973	0.003	−0.010	p6f3 4G 5.5	22 047.39	p5f3d 2H4H2 5.5	193 876.8
582.332	43	4.69E+06	−0.00	582.342	0.003	−0.010	p6f3 4G 4.5	19 969.79	p5f3d 4I6Lb 5.5	191 690.1

(*continued on next page*)

Table 1 (*continued*)

λ_{exp}(Å)	Int_{exp}	$gA(s^{-1})$	CF	λ_{Ritz}(Å)	$\delta\lambda_{Ritz}$(Å)	$\Delta\lambda$(Å)	Lower level label	E_{low}	Upper level label	E_{up}
583.005	19	7.46E+07	0.00	583.005	0.003	0.001	p6f3 2G2 3.5	17 655.11	p5f3d 4I4Gd 4.5	189 180.3
583.451	37	9.82E+07	−0.03	583.459	0.003	−0.008	p6f3 4G 2.5	17 707.17	p5f3d 2H4G2 3.5	189 098.9
587.769	53	9.96E+07	0.00	587.7498	0.0024	0.019	p6f3 4G 4.5	19 969.79	p5f3d 4F6F 4.5	190 110.2
588.260	34	4.54E+06	0.00	588.258	0.003	0.002	p6f3 2I 5.5	30 179.93	p5f3d 4G6Gb 6.5	200 173.3
590.984	21	1.06E+08	0.00	590.980	0.003	0.004	p6f3 4G 4.5	19 969.79	p5f3d 4I4Gd 4.5	189 180.3
595.006	83	4.80E+08	0.02	595.0156	0.0025	−0.009	p6f3 4G 5.5	22 047.39	p5f3d 4F6F 4.5	190 110.2
595.328	20	1.19E+08	0.02	595.322	0.003	0.006	p6f3 2H2 5.5	16 161.53	p5f3d 4I6Ga$_b$ 6.5	184 137.8
596.344D	22	9.55E+07	0.00	596.349	0.003	−0.006	p6f3 2G2 4.5	21 493.39	p5f3d 4I4Gd 4.5	189 180.3
596.344D	22	1.41E+08	0.02	596.355	0.005	−0.012	p6f3 2K 7.5	22 043.77	p5f3d 4F6I 7.5	189 729.0
596.635	45	9.19E+07	0.00	596.639	0.003	−0.004	p6f3 2G2 4.5	21 493.39	p5f3d 2H4G2 3.5	189 098.9
596.660	35	3.37E+07	0.00	596.648	0.003	0.012	p6f3 2H2 5.5	16 161.53	p5f3d 4F6Ha 6.5	183 764.4
598.325	73	3.14E+08	0.02	598.326	0.003	−0.002	p6f3 4G 5.5	22 047.39	p5f3d 4I4Gd 4.5	189 180.3
598.482	92	9.26E+07	0.01	598.493	0.003	−0.011	p6f3 2G2 4.5	21 493.39	p5f3d 4G6Hb 5.5	188 579.7
600.845	21	5.15E+07	−0.01	600.849	0.003	−0.004	p6f3 2H2 5.5	16 161.53	p5f3d 4I6Ga 6.5	182 592.7
602.643	23	4.13E+06	0.00	602.654	0.003	−0.010	p6f3 2G2 3.5	17 655.11	p5f3d 4I2H 4.5	183 587.9
629.894	34	1.67E+08	−0.07	629.901	0.003	−0.007	p6f3 4D 3.5	31 355.04	p5f3d 4F6F 4.5	190 110.2
635.317	26	4.24E+07	0.00	635.303	0.003	0.014	p6f3 2H1 5.5	35 136.61	p5f3d 4I6Lb$_b$ 5.5	192 541.7

p: line resolved on the plate but perturbed by a close line
bl: line partially resolved in a blended emission peak with components of similar intensities; blV means blend by Nd V.
as: asymmetrical line, when the components of the blend have different intensities
D: doubly classified
Lower level label: read $5p^64f^3\ ^4G$ J=5.5 for p6f3 4G 5.5 and so on.
Upper level label: read $5p^54f^35d$ or $5p^54f^36s$ for p5f3d or for p5f3s and $(^4D)^4Fe$ J=4.5 for 4D4Fe 4.5 and so on. p5f3d(s) means a mixed 5d level with a 6s leading component (Cf Table2).

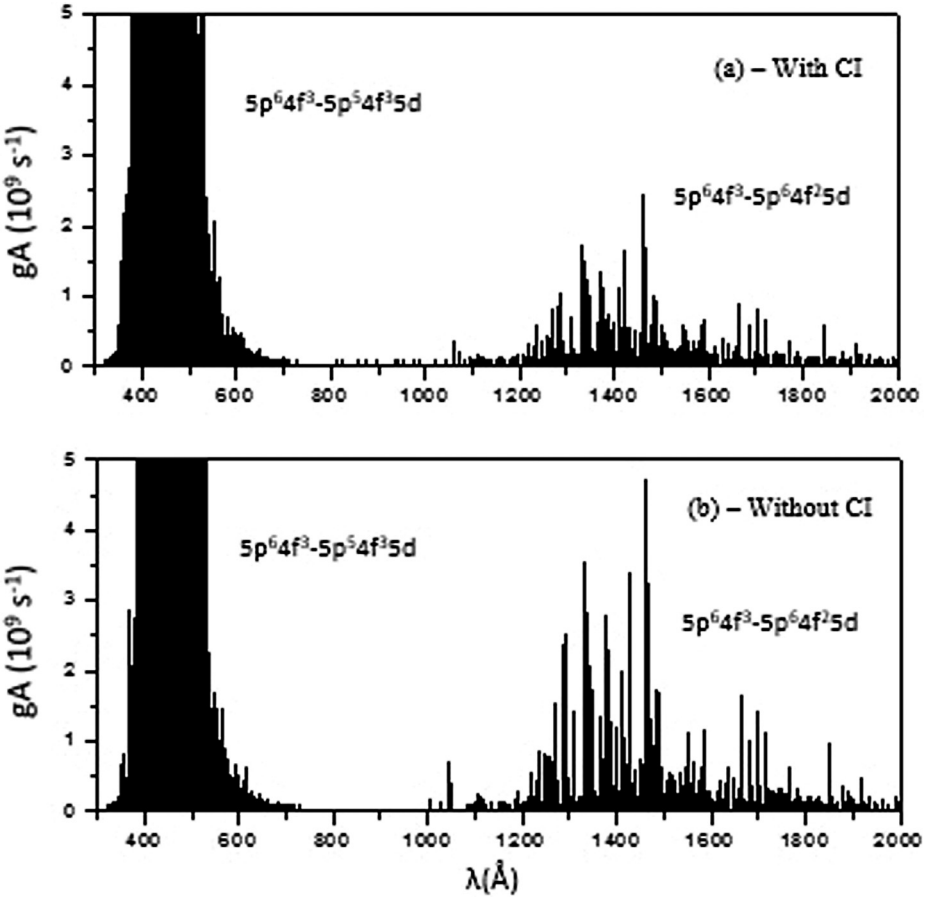

Fig. 2. Reduction of the $5p^64f^3$-$5p^64f^25d$ transition probabilities by the $5p^64f^25d$- $5p^54f^35d$ configuration interaction (with and without including configuration interaction with $5p^54f^35d$). (a) With CI ; (b) Without CI.

Among the 92 parameters, only 5 parameters were left as completely free: the average energies E_{av} of the three configurations $5p^64f^25d$, $5p^64f^26s$ and $5p^54f^35d$, the spin-orbit parameter of the sub-shell 5p, and finally the exchange Slater integral G^1(5p, 5d) which is crucial to fit the gap between the transition arrays at 415 Å and 480 Å. To estimate E_{av} of $5p^54f^35d$, we paid attention to the lower part of the configuration, where many transitions connect the levels to the $5p^64f^3$ ground-state configuration. Its final value of 221 076 cm^{-1} was not far from the adopted value of 221 000 cm^{-1} in [7] (In Table 4 of [7], this number was misprinted in col. 9 instead of col. 10). One may notice that the fitted values of E_{av} are quite different from their HFR values (30 000 cm^{-1}).

Table 2
Even-parity energy levels of the $5p^5 4f^3 5d$ configuration of Nd^{3+}. For each level are given : J, the total angular momentum; E_{exp}, the experimental energy value and its uncertainty (in cm^{-1}); N, the number of transitions involved in its determination; E_{calc}, the calculated energy value from the parametric fit and $\Delta E = E_{exp} - E_{calc}$ (in cm^{-1}); g_L, the calculated Landé factor, the leading LS component of the wavefunction and its percentage as derived from Cowan codes [19]. Two levels of identical first component are distinguished by a subscript "b" for the higher energy level. Levels marked with a " * " belong to the $5p^5 4f^3 6s$ configuration. Two levels of $5p^5 4f^3 5d$ marked by (s) have a first LS component belonging to the $5p^5 4f^3 6s$ configuration.

J	E_{exp} (cm^{-1})	Unc.(cm^{-1})	N	E_{calc} (cm^{-1})	ΔE(cm^{-1})	g_L	1st LS comp.	Perc.
6.5	182 592.7	2.2	4	182 292	301	1.107	(4I) 6Ga	13%
6.5	183 162.8	1.3	2	183 382	−219	1.112	(4I) 4Hf	8%
4.5	183 587.9	2.0	3	183 626	−38	1.048	(4I) 2H	15%
6.5	183 764.4	2.0	3	183 594	171	1.209	(4F) 6Ha	14%
6.5	184 137.8	1.2	3	183 948	190	1.164	(4I) $6Ga_b$	9%
5.5	188 563.0	1.4	2	188 514	49	1.049	(4F) 6I	11%
5.5	188 579.7	1.7	3	189 026	−447	1.136	(4G) 6Hb	9%
3.5	189 098.9	1.8	3	189 028	71	1.153	(2H) 4G2	5%
4.5	189 180.3	0.9	4	188 956	224	1.120	(4I) 4Gd	8%
7.5	189 729.0	2.4	2	189 674	55	1.114	(4F) 6I	14%
5.5	189 995.5	3.0	2	190 098	−103	1.311	(4F) 6F	17%
4.5	190 110.2	1.7	4	190 325	−215	1.202	(4F) 6F	6%
5.5	190 471.1	4.0	2	190 307	164	1.130	(4G) 6Gb	7%
8.5	191 421.6	1.7	1	191 683	−261	1.135	(4I) 4Lc	13%
5.5	191 690.1	3.0	3	191 573	117	1.047	(4I) 6Lb	6%
5.5	192 464.3	1.9	1	192 118	347	1.101	(4I) 4Gd	7%
5.5	192 541.7	1.9	5	192 557	−15	1.034	(4I) $6Lb_b$	7%
7.5	193 028.4	1.8	1	192 962	67	1.101	(2H) 4L2	14%
6.5	193 349.2	2.3	3	193 118	231	1.087	(2K) 4La	5%
6.5	193 876.8	1.9	3	193 564	313	1.158	(2H) 4H2	5%
5.5	195 890.1	3.0	2	196 173	−283	1.104	(2H) 2H2	4%
6.5	196 705.6	1.5	3	197 207	−501	1.177	(4G) 6G	12%
6.5	200 173.3	1.0	5	200 154	20	1.150	(4G) 6Gb	6%
7.5	201 480.7	2.4	2	202 075	−594	1.118	(4F) 6Hb	11%
5.5	201 621.4	1.5	2	201 782	−160	1.125	(4F) 4Gd	4%
6.5	201 674.3	1.1	4	201 813	−138	1.066	(4G) 4Ka	8%
8.5	205 845.6	2.0	2	205 655	191	1.095	(4G) 4Kb	11%
8.5	206 235.2	2.0	1	206 309	−74	1.061	(2L) 4L	13%
7.5	208 806.7	2.1	1	208 523	284	1.033	(4I) 4La	14%
6.5	213 434.6	6.0	2	213 540	−105	1.014	(4I) 4Kb	4%
6.5	216 025.3	1.6	2	216 180	−155	1.012	(2K) 4L	7%
9.5	219 643.5	1.7	1	219 834	−190	1.099	(4I) 2M	18%
9.5	220 514.9	1.8	1	220 460	55	1.047	(2L) 4Ma	28%
8.5	220 933.1	2.2	3	220 327	607	1.081	(4I) 4Ka	7%
8.5	221 559.6	2.0	1	221 375	185	1.069	(4I) $4Ka_b$	5%
5.5	222 663.7	1.9	2	222 599	65	1.091	(2D) 4H2	4%
5.5	224 061.9	4.0	4	223 892	170	1.067	(2H) 2I1	5%
6.5	224 253.6	1.5	3	224 447	−193	1.107	(4F) 6G (s)	7%
7.5	224 288.2	3.0	3	224 654	−366	1.071	(2H) 4K1	8%
7.5	224 949.2	3.0	3	225 273	−324	1.021	(2H) 2L1	9%
6.5	225 925.5	2.0	4	226 088	−163	1.079	(2H) 2I1	7%
4.5	226 942.2	2.0	2	226 950	−8	1.094	(4F) 4Gc	4%
6.5	227 076.0	3.0	4	226 737	339	1.077	(4I) 2Ia	4%
6.5	227 462.5	1.7	5	227 497	−34	1.076	(2L) 4H	12%
5.5	227 724.6	1.8	6	227 666	59	1.053	(2L) 2Ha	7%
8.5	228 554.3	2.3	2	228 538	16	1.033	(2L) 2Lf	10%
6.5	229 397.5	1.3	5	229 205	193	1.073	(2K) 4Hb	6%
8.5	230 894.7	2.0	2	230 591	304	1.011	(2L) 2Md	13%
7.5	231 120.8	4.0	3	231 318	−197	1.028	(2L) 4M	9%
7.5	231 793.5	3.0	4	231 963	−170	1.065	(2G) 2K2	10%
8.5	231 845.6	5.0	2	231 927	−81	1.035	(2K) 2Ma	18%
5.5	232 038.4	1.3	4	231 803	235	1.062	(2G) 4G1	4%
8.5	232 396.0	1.7	2	232 128	268	1.087	(4G) 4Ka	11%
6.5	232 406.2	1.5	3	232 524	−118	1.112	(4G) 4Hc	9%
7.5	232 504.8	1.5	2	232 683	−179	1.108	(2G) 2K1	7%
6.5	232 824.5	2.4	3	232 805	19	1.046	(2G) 2K2	5%
6.5	233 830.6	3.0	3	233 781	49	1.135	(4G) $4Hc_b$	9%
9.5	234 594.7	2.0	1	234 688	−93	1.031	(2L) 2Md	19%
5.5	235 156.4	3.0	3	235 158	−2	1.012	(2I) 4K	7%
8.5	235 332.7	1.5	3	235 217	116	0.990	(2L) 4Na	23%
5.5	235 966.4	3.0	4	235 894	73	1.056	(2K) 4Hb	6%
8.5	236 503.5	5.0	2	236 503	1	0.997	(2L) 4Mb	11%
8.5	237 679.7	3.0	3	237 623	57	1.056	(2K) 4Ka	13%
6.5	237 856.8	1.7	4	238 372	−515	0.996	(2I) 4K	8%
6.5	238 430.3	1.7	3	237 961	470	1.070	(4G) 4Hb	6%
5.5	238 709.0	1.8	3	238 446	263	1.073	(2G) 2H2	6%
7.5	239 094.8	2.1	1	239 129	−34	1.074	(2K) 2Kd	6%
6.5	239 327.9	1.9	5	238 891	437	1.037	(2L) 4L	7%
4.5	239 356.2	3.0	5	239 748	−392	1.047	(4G) 4Ha (s)	5%
9.5	239 521.7	2.1	1	240 122	−600	1.025	(2L) 4Na	33%

(*continued on next page*)

Table 2 (*continued*)

J	E_{exp} (cm^{-1})	Unc.(cm^{-1})	N	E_{calc} (cm^{-1})	$\Delta E(cm^{-1})$	g_L	1st LS comp.	Perc.
8.5	239 666.0	1.7	3	239 400	266	1.054	(2K) 2Mc	14%
7.5	239 778.1	3.0	4	239 794	−16	1.114	(2G) 4I2	7%
6.5	240 040.4	2.3	3	239 965	75	1.040	(2I) 2Ke	5%
7.5	240 670.5	1.5	3	240 786	−115	1.080	(2G) $4I2_b$	11%
6.5	241 212.6	4.0	2	241 149	64	0.991	(4I) 4Ka	11%
4.5	241 974.8	3.0	5	241 922	53	1.022	(2I) 4Gb	3%
8.5	242 279.2	2.3	3	242 248	31	1.061	(2L) 4Ka	11%
5.5	242 534.5	1.9	2	242 538	−4	0.998	(4I) 4If	8%
5.5	242 758.0	3.0	4	242 725	33	1.103	(4D) 4Ga	4%
6.5	242 796.2	1.9	3	243 008	−212	1.010	(2L) 2Ka	6%
7.5	243 032.1	2.5	2	243 079	−47	1.091	(2I) 2Kc	9%
6.5	243 575.6	2.3	2	243 489	86	1.071	(2I) 4Hb	3%
7.5	244 383.4	3.0	2	244 288	95	1.095	(2I) $2Kc_b$	7%
8.5	245 704.8	2.4	2	245 777	−72	1.073	(4I) 4Kd	17%
6.5	247 744.4	2.9	1	247 529	216	1.138	(4I) 4Hc	12%
6.5	247 798.7	2.2	4	247 880	−81	1.079	(4I) 4Kb *	9%
5.5	253 568.5	2.2	2	253 419	149	1.044	(2F) 4I1	6%
4.5	254 434.6	2.1	3	254 806	−371	1.130	(4F) 4Gd	13%
4.5	260 470.3	4.0	3	260 153	318	1.051	(2G) 4H2	5%
7.5	260 809.0	3.0	1	260 684	125	0.946	(2K) 2Ld	26%
6.5	261 522.8	3.0	3	261 161	362	0.998	(2K) 2Ke	16%
3.5	261 585.0	2.4	2	261 182	403	1.018	(4G) 4Ge	8%
7.5	262 050.0	3.0	1	262 001	49	1.060	(2K) 2Ke	29%
8.5	262 377.5	2.9	1	262 762	−384	1.050	(2K) 2Ld	37%
3.5	262 535.2	3.0	2	262 780	−245	1.114	(4G) 4Ff	11%
5.5	262 910.4	1.9	3	263 251	−341	1.176	(4G) 4Ge	14%
6.5	263 107.0	3.0	1	262 892	215	1.190	(4G) 4Hd	26%
5.5	263 215.7	4.0	2	263 730	−515	1.025	(2K) 2If	18%
4.5	264 511.1	3.0	3	264 464	47	1.225	(4G) 4Fc	16%
3.5	264 862.0	3.0	1	265 132	−270	1.081	(2D) 2F1	13%
3.5	271 108.5	2.3	2	271 172	−64	1.160	(4D) 4Fe	6%
7.5	271 194.2	2.1	2	270 940	255	1.015	(2L) 2Le	16%
5.5	271 396.5	2.9	1	271 013	383	1.049	(2I) 2Ie	11%
4.5	272 387.5	2.2	3	272 741	−354	1.000	(2I) 2Hf	26%
8.5	272 514.9	5.0	2	272 680	−165	0.991	(2L) 2Me	22%
3.5	272 617.7	5.0	2	272 664	−46	1.293	(4D) 4Df	11%
8.5	272 626.1	2.1	2	272 536	90	1.017	(2L) 2Le	20%
6.5	272 899.7	2.2	2	273 050	−150	0.984	(2I) 2Kd	15%
7.5	272 938.4	2.4	2	272 761	178	1.062	(2I) 2Kd	34%
9.5	273 532.0	3.0	1	273 873	−341	1.048	(2L) $2Md_b$	36%
5.5	273 678.6	2.1	2	274 160	−481	1.061	(2I) 2Hf	21%
4.5	273 770.7	3.0	2	273 831	−60	1.261	(4D) 4Fe	20%
6.5	273 912.9	2.4	2	273 961	−48	1.090	(2I) 2Ie	16%
2.5	276 425.4	2.9	1	276 146	279	0.991	(2D) 2F2	18%
5.5	277 312.8	3.0	3	277 076	237	1.059	(2H) 2H1	12%
4.5	277 426.8	3.0	2	277 150	277	0.988	(2H) 2H1	8%
7.5	277 550.8	3.0	2	277 201	350	1.033	(2L) 4L *	14%
2.5	277 827.9	2.1	2	277 542	286	1.061	(2D) 2D2	10%
5.5	278 270.7	5.0	3	278 374	−104	1.027	(2H) $2I1_b$	8%
6.5	278 497.2	3.0	2	278 382	115	1.054	(2H) $2I1_b$	22%
4.5	278 631.0	3.0	1	278 635	−4	1.050	(2H) 2G1	12%
1.5	283 605.0	3.0	1	283 321	284	0.968	(2F) 2D1	17%
2.5	284 327.7	3.0	1	284 464	−137	1.184	(2F) 2D1	19%
4.5	284 421.0	3.0	1	284 453	−32	1.113	(2F) 2G1	20%
4.5	292 989.0	3.0	1	293 011	−22	1.098	(2G) 2G2	14%

Read (^{4}I) ^{6}Ga for (4I) 6Ga and so on.

This is often the case in lanthanide ions. As discussed in [10], these differences are likely due to an underestimation of the core-polarization by external electrons in the HFR calculations. All the effective parameters except β and γ were fixed to their final fitted values from the previous Nd IV study [7]. It was also the case for the exchange parameter G^3 (fs). Constraints were applied to other parameters as indicated in Table 3 by linking their ratios according to the values appropriately chosen from other lanthanide ions. All the CI parameters were linked by the same ratio to their HFR values (SF) and varied as one single parameter. The SF's final value of 0.72 is larger than the value of 0.634 determined in [7], but close to the value of 0.719 found in Nd V [13]. The present value is more reliable since the fit included experimental level energies of $5p^54f^35d$ previously unknown. As for the parameters related to the basically unknown $5p^54f^36s$ configuration (only three experimental levels), their values were fixed by adopting the initial scaling factors from the $5p^54f^35d$ configuration except for G^3 (fs), which SF was adopted from the $5p^64f^26s$ configuration. Overall the number of equivalent free parameters was 19. The root mean square deviation of the fit was 184 cm^{-1}.

The parameters of Table 3 were used for a final diagonalization by RCG that resulted in the calculated energies (E_{calc}), the Landé factors (g_L) and the level compositions by the first LS components reported in Table 2. The resulting gA and CF values are listed in Table 1. Although there are many |*CF*| less than or equal to 0.01, which means severe cancellation effects [24], they do not

Table 3
Fitted parameters and Hartree-Fock integrals (in cm^{-1}) of even-parity configurations of Nd^{3+}. Unc. (in cm^{-1}) are the uncertainties of the parameters from the fit. Constraints on parameters are denoted by 'f' (fixed) or 'r' (linked ratios). The scaling factor SF = P_{fit}/P_{HFR}, except for the average energy E_{av} where P_{fit} - P_{HFR} is given. For the unknown $5p^54f^36s$ configuration, the column "Adop." gives the parameter values adopting the initial SF from $5p^54f^35d$, except for G^3(fs), which SF is adopted from $5p^64f^26s$.

	$5p^64f^25d$				$5p^64f^26s$				$5p^54f^35d$				$5p^54f^36s$		
Param. P	P_{fit}	Unc.	P_{HFR}	SF	P_{fit}	Unc.	P_{HFR}	SF	P_{fit}	Unc.	P_{HFR}	SF	Adop.	P_{HFR}	SF
E_{av}	90 146	106	55 887	34 259	123 058	52	90 977	32 081	221 076	22	196 424	24 652	252 021	226 039	25 982
F^2(ff) r1	84 092	183	109 950	0.765	83 412	181	110 707	0.753	80 394	175	104 121	0.772	80 848	104 997	0.770
F^4(ff) r2	60 125	624	69 359	0.867	60 575	629	69 878	0.867	54 372	565	65 415	0.831	55 450	66 012	0.840
F^6(ff) r3	40 495	485	50 007	0.810	40 795	488	50 392	0.810	37453	448	47 084	0.795	38 022	47 527	0.800
α	20	f			20	f			22	f			22		
β r4	−556	−96			−556	−96			−553	−96			−557		
γ r5	1291	115			1291	115			1887	168			1817		
ζ_f r6	987	12	1052	0.938	993	12	1059	0.938	901	11	972	0.926	908	979	0.927
ζ_{5p}									17 360	88	17 350	1.001	17 803	17 803	1.000
ζ_{5d} r7	1129	26	1146	0.985					1028	24	1047	0.982			
F^2(fp)									34 443	570	51 787	0.665	36 682	52 403	0.700
F^1(fd)	758	f							758	f					
F^2(fd) r8	23 442	204	30 830	0.760					22 110	192	30 248	0.731			
F^3(fd)	149	f							149	f					
F^4(fd) r9	16 745	435	15 288	1.095					17 247	449	15 161	1.138			
F^2(pd)									40 350	f	49 630	0.813			
G^2(fp)									22 829	f	27 437	0.832	22 939	27 570	0.832
G^4(fp)									15 873	f	21 226	0.748	16 018	21 415	0.748
G^1(fd) r10	11 626	112	13 343	0.871					11 152	108	14 201	0.785			
G^2(fd)	2012	f							2012	f					
G^3(fd) r11	10 759	351	11 355	0.948					11 632	379	11 677	0.996			
G^4(fd)	1757	f							1757	f					
G^5(fd) r12	6868	337	8788	0.782					7334	360	8956	0.819			
G^1(pd) r13									38 791	64	58 080	0.668			
G^3(pd) r13									28 455	48	36 257	0.785			
G^3(fs)					2732	f	3365	0.812					2847	3506	0.812
G^1(ps)													6336	6336	1.000

CI param.	P_{fit}	Unc.	P_{HFR}	SF
$5p^64f^25d$-$5p^64f^26s$				
R^2(fd.fs) r14	702	21	974	0.72
R^3(fd.sf) r14	2136	62	2962	0.72
$5p^64f^25d$-$5p^54f^35d$				
R^2(fp.ff) r14	−13 651	−402	−18 934	0.72
R^4(fp.ff) r14	−7281	−214	−10 099	0.72
R^2(pp.fp) r14	−27 124	−799	−37 622	0.72
R^2(pd.fd) r14	−19 289	−568	−26 754	0.72
R^4(pd.fd) r14	−12 210	−360	−16 936	0.72
R^1(pd.df) r14	−17 931	−528	−24 870	0.72
R^3(pd.df) r14	−12 494	−368	−17 330	0.72
$5p^64f^25d$-$5p^54f^36s$				
R^2(pd.fs) r14	3799	112	5275	0.72
R^1(pd.sf) r14	1687	50	2342	0.72
$5p^64f^26s$-$5p^54f^35d$				
R^2(ps.fd) r14	4670	138	6481	0.72
R^3(ps.df) r14	−1000	−29	−1384	0.72
$5p^64f^26s$-$5p^54f^36s$				
R^2(fp.ff) r14	−13 546	−399	−18 809	0.72
R^4(fp.ff) r14	−7218	−213	−10 022	0.72
R^2(pp.fp) r14	−27 204	−801	−37 774	0.72
$5p^54f^35d$-$5p^54f^36s$				
R^2(fd.fs) r14	109	3	152	0.72
R^3(fd.sf) r14	1900	56	2639	0.72
R^2(pd.ps) r14	−9178	−270	−12 744	0.72
R^1(pd.sp) r14	−3414	−101	−4739	0.72

affect the reliability of the present determination of energy levels. Fig. 2 (a) and (b) display the values of gA of the transition array $5p^64f^3$ - $5p^64f^25d$ calculated respectively with and without the $5p^54f^35d$ - $5p^64f^25d$ configuration interaction (CI) and they illustrate the reduction of transition probabilities by a factor of about two for the $5p^64f^3$ - $5p^64f^25d$ resonance transition array. This reduction was predictable from the previous Nd IV parametric studies [7,9] with an estimated E_{av} for the then unknown configuration $5p^54f^35d$. However, the newly fitted parameter values, including the CI parameters, derived from the precise knowledge of energy levels in the $5p^54f^35d$ configuration, show a noticeable influence on the calculated gA values of resonance lines. Fig. 3 displays a comparison between the gA values as derived from the present parametric study and the values from previous studies [7,9] for all the observed resonance lines [7]. The present gA values show a smooth reduction of 11% in average compared with the values from [7] using the same configuration basis, whereas their ratios to values calculated with a larger basis [9] have an average close to 1, in spite of more scattered differences. This comparison confirm the reliability of the present gA values.

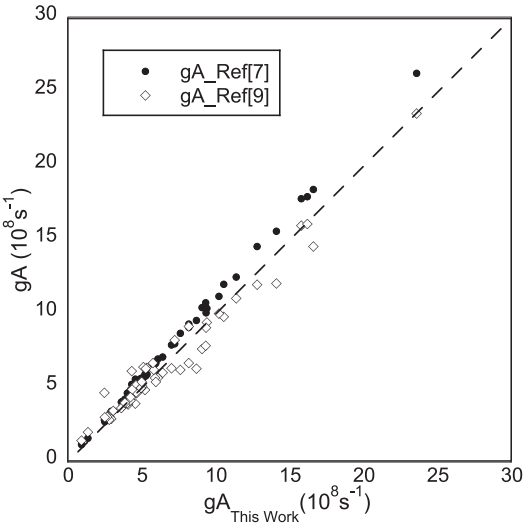

Fig. 3. Comparison between gA from the present work and gA from the previous studies [7,9] for the $5p^64f^3$-$5p^64f^25d$ transitions. In the previous parametric studies, with a larger configuration basis in [9] than in [7], the parameters for the unknown interacting configuration $5p^54f^35d$ were fixed to estimated values. In the present work, they have values fitted with experimentally determined energy levels.

5. Conclusion

We have extended the analysis of the Nd IV spectrum by classification of 313 spectral lines in the wavelength region of 397–636 Å leading to the determination of 125 previously unknown energy levels belonging all but two to the core-excited configurations $5p^54f^35d$. The parametric interpretation of the even configurations including these new experimental levels allowed a more exact description of the $5p^64f^25d$ -$5p^54f^35d$ configuration interaction and its reduction effect upon the transition probabilities of the transition array $5p^64f^3$-$5p^64f^25d$. At the end of the present work, the lowest part of the $5p^54f^35d$ configuration, mostly consisting of sextuplet states, stays unknown. Indeed, due to the insufficient breakdown of LS coupling in these levels, their transitions to the ground configuration $5p^64f^3$, comprising only doublets and quartets, have too small probabilities to be identified in the experimental line list.

Acknowledgements

We are thankful to Dr N. Spector for providing us the spectrogram earlier recorded at the NBS by himself and late Dr J. Sugar, similarly to the ones already used in the previous Nd V analysis [13]. Supports from Université Mouloud Mammeri, Tizi-Ouzou, Algeria and from the project A25N01UN150120150001, CNEPRU, Algeria are acknowledged. Financial supports from the French CNRS - PNPS national program and from the Paris Observatory Federal Action "Stars" (AFE) are acknowledged. This work is also part of the Plas@Par LabEx project managed by the French ANR (ANR-11-IDEX-0004-02).

References

[1] Martin W. C., Zalubas R., Hagan L.. Atomic energy levels - The Rare-Earth elements. NSRDS-NBS (US), 60, 1978 (1978).
[2] Kramida A., Ralchenko Y., Reader J., NIST ASD Team. NIST Atomic Spectra Database (ver. 5.5.6), [Online]. Available: https://physics.nist.gov/asd [2017, April 9]. National Institute of Standards and Technology, Gaithersburg, MD.; 2018.
[3] Bünzli J-C, Comby S, Chauvin A-S, Vandevyver C. New opportunities for lanthanide luminescence. J Rare Earths 2007;25:257–74.
[4] Ryabchikova T, Ryabtsev A, Kochukhov O, Bagnulo S. Rare-earth elements in the atmosphere of the magnetic chemically peculiar star HD 144897. New classification of the Nd III spectrum. Astron Astrophys 2006;456:329–38. arXiv: astro-ph/0604546, doi: 10.1051/0004-6361:20065367.
[5] Kasen D, Badnell NR, Barnes J. Opacities and spectra of the r-process ejecta from neutron star mergers. Astrophys J 2013;774. arXiv: 1303.5788, doi: 10.1088/0004-637X/774/1/25.
[6] Wyart J-F, Meftah A, Bachelier A, Sinzelle J, Tchang-Brillet W-ÜL, Champion N, et al. LETTER TO THE EDITOR: Energy levels of $4f^3$ in the Nd^{3+} free ion from emission spectra. J Phys B Atomic Mol Phys 2006;39:L77–82. doi:10.1088/0953-4075/39/5/L01.
[7] Wyart J-F, Meftah A, Tchang-Brillet W-ÜL, Champion N, Lamrous O, Spector N, et al. Analysis of the free ion Nd^{3+} spectrum (Nd IV). J Phys B Atomic Mol Phys 2007;40:3957–72. doi:10.1088/0953-4075/40/19/013.
[8] Meftah A, Wyart J-F, Sinzelle J, Tchang-Brillet W-ÜL, Champion N, Spector N, et al. Spectrum and energy levels of the Nd^{4+} free ion (Nd V). Phys Scr 2008;77(5). doi:10.1088/0031-8949/77/05/055302.
[9] Enzonga Yoca S, Quinet P. Relativistic Hartree-Fock calculations of transition rates for allowed and forbidden lines in Nd IV. J Phys B Atomic Mol Phys 2014;47(3). doi:10.1088/0953-4075/47/3/035002.
[10] Dzuba VA, Safronova UI, Johnson WR. Energy levels and lifetimes of Nd IV, Pm IV, Sm IV, and Eu IV. Phys Rev A 2003;68(3). doi:10.1103/PhysRevA.68.032503.
[11] Meftah A, Wyart J-F, Champion N, Tchang-Brillet W-ÜL. Observation and interpretation of the Tm^{3+} free ion spectrum. Eur Phys J D 2007;44:35–45. doi:10.1140/epjd/e2007-00173-x.
[12] Reader J, Wyart J-F. Observation of inner-shell-excited configurations in triply ionized cerium Ce^{3+}. Phys Rev A 2009;80(4). doi:10.1103/PhysRevA.80.042517.
[13] Deghiche D, Meftah A, Wyart J-F, Champion N, Blaess C, Tchang-Brillet W-ÜL. Observation of core-excited configuration in four-time ionized neodymium Nd^{4+} (Nd V). Phys Scr 2015;90(9). doi:10.1088/0031-8949/90/9/095402.
[14] Meftah A, Wyart J-F, Tchang-Brillet W-ÜL, Blaess C, Champion N. Spectrum and energy levels of the Yb^{4+} free ion (Yb V). Phys Scr 2013;88(4). doi:10.1088/0031-8949/88/04/045305.
[15] Kelly RL. Atomic and ionic spectrum lines below 2000 angstroms. hydrogen through krypton. J Phys Chem Ref Data 1987;16:1.
[16] Ryabtsev AN, Kononov EY, Kildiyarova RR, Tchang-Brillet W-ÜL, Wyart J-F. The spectrum of seven times ionized tungsten (W VIII) relevant to tokamak divertor plasmas. Phys Scr 2013;87(4). doi:10.1088/0031-8949/87/04/045303.
[17] Kramida A. Energy levels and spectral lines of quadruply ionized iron (Fe V). Astrophys J Suppl Ser 2014;212. 11, doi: 10.1088/0067-0049/212/1/11.
[18] Wyart J-F. On the interpretation of complex atomic spectra by means of the parametric Racah-Slater method and cowan codes. Can J Phys 2011;89:451–6. doi:10.1139/p10-112.
[19] Cowan R. The theory of atomic structure and spectra. Los Alamos series in basic and applied sciences. University of California Press; 1981. ISBN 9780520906150. https://books.google.fr/books?id=tHOXLrXkJRgC.
[20] Kramida A.. A suite of atomic structure codes originally developed by R. D. Cowan adapted for Windows-based personal computers.National Institute of Standards and Technology, (Accessed: 2018-10-15); doi:10.18434/T4/1502500.
[21] Azarov VI. Formal approach to the solution of the complex-spectra identification problem. I. theory. Phys Scr 1991;44:528–38. doi:10.1088/0031-8949/44/6/004.
[22] Azarov VI. Formal approach to the solution of the complex-spectra identification problem. 2. implementation. Phys Scr 1993;48:656–67. doi:10.1088/0031-8949/48/6/004.
[23] Kramida AE. The program LOPT for least-squares optimization of energy levels. Comput Phys Commun 2011;182:419–34. doi:10.1016/j.cpc.2010.09.019.
[24] Biémont É. Recent advances and difficulties in oscillator strength determination for Rare-Earth elements and ions. Phys Scr Vol T 2005;116:55–60. doi:10.1088/0031-8949/2005/T119/010.